GKSS
FORSCHUNGSZENTRUM
in der HELMHOLTZ-GEMEINSCHAFT

Baltic Holocene Climate and regional sea-level change: A statistical analysis of observations, reconstructions and simulations within present and past as analogues for future changes

Authors:
B. Hünicke
E. Zorita
S. Haeseler

ISSN 0344-9629

HELMHOLTZ
| GEMEINSCHAFT

wissen
schafft
nutzen

GKSS 2010/2

GKSS 2010/2

Baltic Holocene Climate and regional sea-level change: A statistical analysis of observations, reconstructions and simulations within present and past as analogues for future changes

Authors:

B. Hünicke

E. Zorita

(Institute of Coastal Research)

S. Haeseler

**(current address:
Deutscher Wetterdienst,
Bernhard-Nocht-Straße 76,
20359 Hamburg, Germany)**

GKSS-Forschungszentrum Geesthacht GmbH · Geesthacht · 2010

Die Berichte der GKSS werden kostenlos abgegeben.
The delivery of the GKSS reports is free of charge.

Anforderungen/Requests:

GKSS-Forschungszentrum Geesthacht GmbH
Bibliothek/Library
Postfach 11 60
21494 Geesthacht
Germany
Fax.: +49 4152 87-17 17

Als Manuskript vervielfältigt.

ISSN 0344-9629

GKSS-Forschungszentrum Geesthacht GmbH · Telefon (04152) 87-0
Max-Planck-Straße 1 · 21502 Geesthacht / Postfach 11 60 · 21494 Geesthacht

GKSS 2010/2

Baltic Holocene Climate and regional sea-level change: A statistical analysis of observations, reconstructions and simulations within present and past as analogues for future changes

Birgit Hünicke, Eduardo Zorita and Susanne Haeseler

70 pages with 29 figures and 7 tables

Abstract

The study presents the analysis of regional climate drivers and their contribution to Baltic sea-level variations over the past decades to millennia, and into the next decades. In the previous project SINCOS, the relationships between some regional driving factors, such as temperature, wind and precipitation on the one hand and Baltic Sea level on the other hand, had been analysed. This allowed to establish statistical transfer functions between the regional drivers and sea-level. In the present project these transfer functions were applied to long Holocene climate simulations with the state-for-the-art climate model ECHO-G, covering the last 7000 years, and also to scenario simulations for the 21st century. The results confirmed that regional climate contributions from wind and precipitation are of the order of a few mm/year. Thus, although they are smaller than the geologic contribution during the Holocene period, they must be taken into account taking when estimating regional sea-level rise resulting from anthropogenic climate change.

The analysis of the climate model simulations and their application to a transfer function between climate forcings and sea level, clearly pointed out that present global and regional climate models are hindered by their limited resolution and limited representation of regional components. Thus, efforts to design regional atmosphere-coupled models for the Baltic Sea region would benefit greatly.

In parallel to the above, a set of dendroclimatological data sets was compiled for the Baltic Sea Area and analysed in terms of its utility for the study of its relationship to sea-level variations. The majority of proxy data available for model-proxy comparison in this region mostly allow for a reconstruction of past summer temperatures, and are therefore not useful to infer past sea-level variations. However, they offer a background to which climate simulation can be compared. Such an effort could be made for a time period covering the last 500 years. An extension of valuable proxy data time series to cover the winter half year should be a future focus to ascertain the realism of climate models to simulate climate changes at centennial and millennial timescales.

Regionale Klima- und Meeresspiegeländerungen der Ostsee im Holozän: Eine statistische Analyse von Beobachtungen, Rekonstruktionen und Simulationen der Gegenwart und Vergangenheit als Analoga für zukünftige Änderungen

Zusammenfassung

Die vorliegende Studie analysiert den Einfluss regionaler Klimafaktoren auf Wasserstandsänderungen der Ostsee in Gegenwart, Vergangenheit und Zukunft auf Zeitskalen von Jahrzehnten bis zu Jahrtausenden. Basierend auf statistischen Transferfunktionen konnten Abschätzungen des regionalen Beitrages von Wind (für die zentrale und nördliche Ostsee) und Niederschlag (für die südliche Ostsee) getroffen werden. Dieser Beitrag bewegt sich in einer Größenordnung von einigen Millimetern/Jahr und sollte in der Abschätzung zukünftiger regionaler Meeresspiegeländerungen Berücksichtigung finden. Als Datengrundlage der Studie dienten neben den Pegeldaten der Ostsee, Klimazeitserien aus Beobachtungen und Reanalysen, sowie Langzeit-Klimasimulationen über die letzten 7000 Jahre mit dem globalen gekoppelten Atmosphäre-Ozean Modell ECHO-G und IPCC AR4 Zukunftsszenarienrechnungen für das 21. Jahrhundert. Die Analyse der Klimasimulationen fokussierte auf die Faktoren Luftdruck, Temperatur, Niederschlag sowie Wind. Zudem wurde ein auf Baumringdaten basierender dendroklimatologischer Datensatz für die Ostsee zusammengestellt und dessen Anwendbarkeit auf die formulierte Transferfunkion (Klima→Wasserstand) geprüft. Die Mehrheit der zur Verfügung stehenden Baumringdaten erlaubte nur eine Rekonstruktion von Sommertemperaturen, jedoch nicht der benötigten Wintertemperaturen. Mit Hilfe der Klimamodelldaten konnten die aus Proxy-Daten gewonnenen Informationen, auf Basis statistischer Verfahren für den Zeitraum der letzten 500 Jahre, für die Temperatur zusammengeführt werden. Eine weitere Erhöhung der aus Baumringen gewonnenen Proxy-Datendichte sollte angestrebt werden, um die Grenzen und Möglichkeiten von Langzeitklimasimulationen über Jahrhunderte bis Jahrtausende besser abschätzen zu können.

Manuscript received / Manuskripteingang in TFP: 09. Februar 2010

Contents

1 Introduction

The study presents a continuation of a research work started in 2003 within the DFG Research Unit SINCOS (acronym CLIMLEVEL), which has focused on the estimation of the influence of regional climate factors on Baltic Sea level variations. For this purpose, statistical transfer functions linking sea-level records with regional climate variables have been developed and tested in the past two centuries, using climate reconstructions and available long sea-level records. Climate simulations with global climate models of the Late Holocene and of the 21st century where then regionalized using these transfer functions. The results, summarised from Hünicke and Zorita in *Berichte der Römisch-Germanischen Komission* (2007), indicated that regional climate factors cannot be neglected and need to be, at least in principle, taken into account in the estimation of future, and past, sea-level variations.

Within the DFG project cluster SINCOS II (acronym CLIMLEVEL-2) we extended this type of analysis to longer timescales, covering the last 7000 years of the Holocene. For this purpose, very long climate simulations with the state-of-the-art climate model ECHO-G, performed recently within the paleoclimate group of GKSS, were analysed for our region of interest –the Baltic Sea Area. In parallel, dendroclimatological data sets of the Baltic Area were collected and analysed in terms of their utility for the study of their relationship to sea-level variations.

All in all, the project focused on a number of challenging research questions regarding the instrumental (observational) record but also global climate simulations and proxy-data. Consequentially, the report is structured in three main Research Foci, regarding (a) the observational period, (b) climate model simulations and (c) proxy data. Within the report, the following main questions are posed and tried to be addressed: Is it possible to identify the underlying influence of regional climate factors by analysing the amplitude of the annual cycle of sea-level, which is not affected by the isostasy? What can we learn from climate model simulations of Baltic Sea-level variations over the past decades to millennia's for future times? What is the best proxy data in the Baltic Sea Sector to ascertain the realism of the Holocene climate model simulations and how useful is this data for the particular needs of climate modelling within the Baltic Sea Region? Thus, the presented study delivers not just

new datasets, but also new and promising findings for the Baltic Sea Research Community.

The work is structured as follows: In Chapter 2 all relevant data sets used for this study are presented, including sea-level and climate observations, climate reconstructions/ proxy data and climate model simulations. As the climate simulations with ECHO-G form one of the key foci, they are presented in more detail, including also a description of the external forcing factors. To do so, in Chapter 3 firstly the establishment of statistical approaches in the observational period is presented by the application of two different strategies, that is to say a statistical downscaling and a trend analysis. In a next step, in Chapter 4 the global climate model simulations were evaluated for the Baltic Sea and the results of the ECHO-G climate simulations (Millennia and Holocene Simulations), which were performed at GKSS, were presented with a special focus on the Baltic Sea Region. Here, special interest was devoted to the simulated temperature, precipitation, sea-level pressure (SLP; including the North Atlantic Oscillation (NAO)) and the simulated wind time series. While the first three form the key factors for the analysis of the relationship between climate influence and sea-level variations, the latter one is of high importance for the hydrodynamic modelling within SINCOS II, which was performed by our project partners of IOW. This is followed by the application of the statistical approaches, found in the observational period, to the output of global climate model simulations, to estimate the contribution of the regional climate drivers to winter Baltic sea-level changes. This estimation was done for past winter sea-level changes as well as for future winter sea-level changes. Chapter 5 deals proxy data with a special focus on tree ring data sets. Tree ring data sets with relevance for the Baltic Sea Region as well as climatic datasets with relevance for this tree ring data sets are presented and discussed. The datasets were statistically evaluated and standardised by specific software programs, resulting in the establishment of chronologies. The evaluation of the raw ring width data is discussed and climatic signals within the tree ring data are identified with a special focus on temperature and precipitation conditions. Chapter 6 presents a Summary of the results and an outlook.

2 Data sets

In this study the main focus lies on the winter season, which is defined here as the mean of the month December, January, February (DJF). As the timescales of our interest are decadal, since future climate change will presumably evolve at these slow timescales, all time series were smoothed with an 11-year running mean filter.

2.1 Baltic sea-level observations

For analyses in the 20th century data from 30 Baltic Sea tide gauge stations from the Revised Local Reverence (RLR) dataset of the Permanent Service for Mean Sea Level (PSMSL; Woodworth and Player 2003) was used. For the analysis back to 1800 the four longest sea-level records from stations situated along the Baltic Coast, Kolobrzeg (PSMSL, and updated by Technische Universität Dresden), Swinoujscie (PSMSL), Stockholm (Ekman 2003) and Kronstadt (Bogdanov et al. 2000) have been selected. Fig. 1 shows the location of the sea-level gauges.

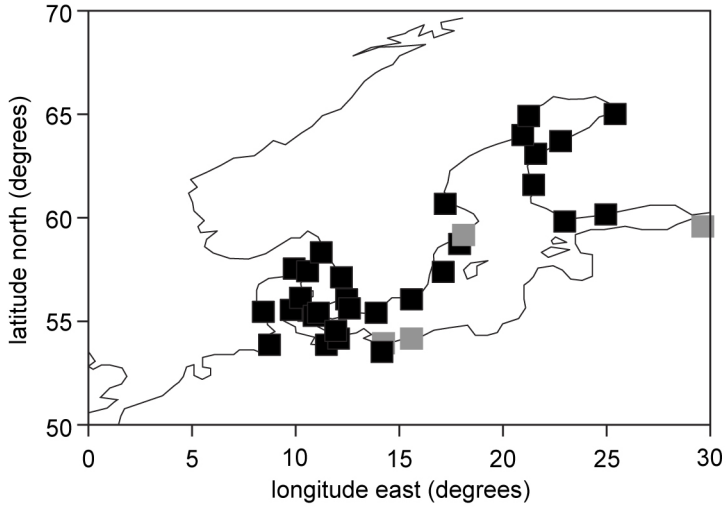

Fig. 1: *Sketch of the Baltic Sea, showing the location of the sea-level gauges. The grey squares indicating the four longest available sea-level records (from Hünicke and Zorita 2008).*

The observation records contain a trend which is caused by a combination of postglacial land uplift and eustatic sea-level change. On the time scales of our analysis this trend is assumed to be linear and is eliminated by statistically estimating the linear trend and subtracting it from each sea-level record. As we are interested in the regional climate factors that may drive sea-level variations, we therefore focus on the inter-annual and decadal variations around this long-term trend.

2.2 Climatic data sets

2.2.1 Observational and climate data from Reanalysis

The following gridded climatic data sets were used in this study:

- 5°x5° monthly mean SLP from the National Centre of Atmospheric Research (NCAR, Trenberth and Paolino 1980) for the geographical region 30°W to 40°E; 30°-70°N
- 0.5°x0.5° monthly precipitation means from Mitchell and Jones (2005) for the geographical region 11°-26°E; 52-62°N.

These observational datasets coincide with the calibration period of the corresponding *climate reconstructions* (see Section 2.2.2). The geographical distribution of these climate data sets was selected based on the following climate data sets used by Hünicke and Zorita (2006):

- 5°x5° monthly mean sea-level-pressure (SLP) from the National Centre for Atmospheric Research (NCAR, Trenberth and Paolino 1980) for the region 70W to 40E and 15N to 85N,
- 2.5°x3.75° monthly precipitation totals from the Climate Research Unit (CRU) (Hulme et al. 1998) for the region 11.25E to 26.25E and 52.5 N to 62.5 N.

2.2.2 Climate reconstructions

The last 200 years of long gridded winter climate reconstructions, based on early instrumental station series (pressure, temperature and precipitation) and documentary data (not including sea-level data) from Eurasian sites have been extracted for our region of interest:

- 5°x5° sea-level pressure fields (Luterbacher et al. 2002) for the region 30W-40E; 30-70N
- 0.5°x0.5° precipitation reconstructions (Pauling et al. 2006) for the region 11-26E and 52-62N.

The climate reconstructions coincide with corresponding observations in their calibration period. An important aspect of these climate reconstructions is that they are not simple spatial interpolation of available long-instrumental and indirect (documentary, proxy-based) climate data and the reconstruction method is based on principal component regression. More details about data and methods can be found in the original references.

2.2.3 Climate model data

The key focus of the presented study lies on the analysis of the output of Holocene climate simulations, which were performed with the coupled atmosphere-ocean General Circulation Model (GCM) ECHO-G (Legutke and Voss 1999) at our Paleoclimate Research Group at GKSS within the last years. For that reason, the climate model, the experimental set up of the simulations as well as the different external forcings (depending on the length of the simulation) will be presented in the following in more detail.

2.2.3.1 The climate model ECHO-G

The coupled GCM ECHO-G consists of the atmospheric component (AGCM) ECHAM4 (Roeckner et al. 1996) with a horizontal resolution of T30 (approximately 3.75°x3.75°) and 19 vertical levels (five of them located above 200mb) and the ocean component (OGCM) HOPE-G (Wolff et al. 1997) with a T42 improved equatorial resolution (horizontal resolution is about 2.8°x2.8°) and 20 vertical levels. Both of the sub-models have been developed at the Max Planck Institute for Meteorology (MPI-M) in Hamburg.

2.2.3.2 Climate simulations performed at GKSS and their External Forcings

For the simulations carried out by GKSS, the model time step was 30 minutes and the data was stored each 12 model-hours. For the performed climate simulations different external forcings had to be considered. Fig. 2 and Fig. 3 give an overview about the different climate simulations and the respective external forcings.

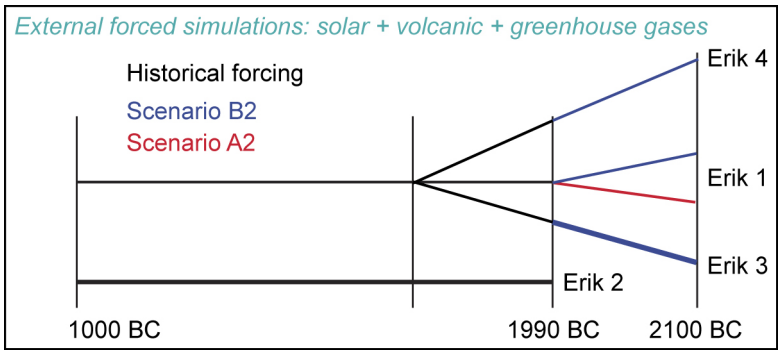

Fig. 2: *Millenium Climate Simulations (990-1990 AD) performed with ECHO-G. Externally forced by solar, volcanic and greenhouse gases. Starting with warm ocean (Erik 1) and cold ocean (Erik 2) as initial conditions.*[1] *Erik 1 was continued until 2100, driven by IPCC SRES scenarios A2 and B2. Erik 3 and Erik 4 were branched out from Erik 1 in year 1756 and continued until 2100 under scenario B2.*

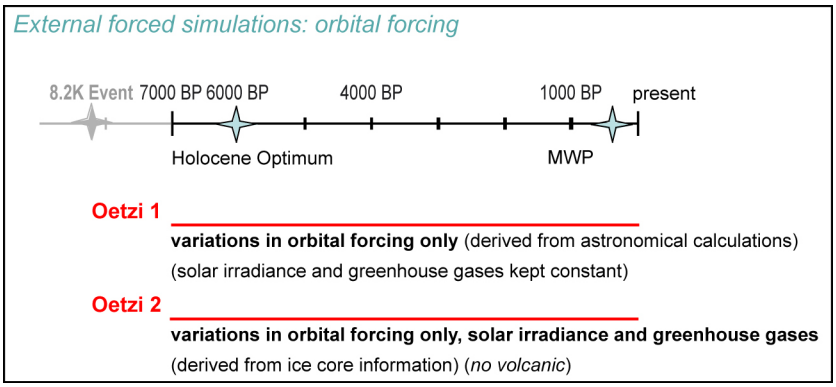

Fig. 3: *Holocene Climate Simulations (7000 BP -1998 AD) performed with ECHO-G. Externally forced by orbital, solar and greenhouse gases (Oetzi 1) (no volcanic) and only orbital forcing (Oetzi 2).*[2]

[1] The Millenium Simulation is named after Erik the Red (950–c. 1003), who founded the first Nordic settlement in Greenland.

[2] The Holocene simulation is named after the around 5300 years old Glacier mummy Oetzi.

For the simulation of the last millennium (Erik) estimations of the changes in the effective solar constant (variations in the solar constant and volcanoes) and greenhouse gases (CO2, CH4, N2O) were considered. The external forcings used in this climate simulations are shown in Fig. 4 (external forcings Erik), together with the global temperature response in the simulations starting in 1000 A.D. and 1500 A.D. (middle panel) and 100-year running temperature trends (lower panel).

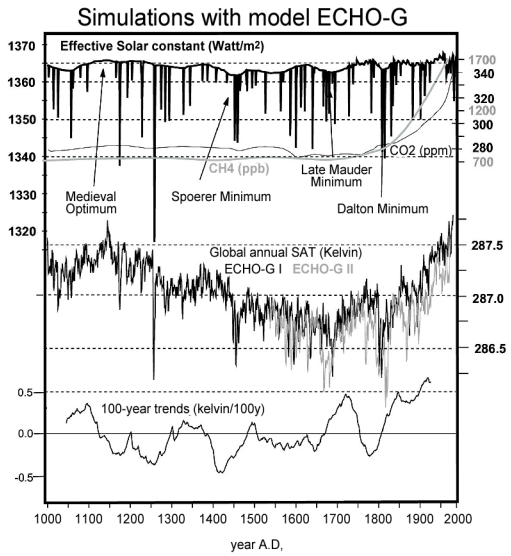

Fig. 4: *External forcing used in the ECHO-G climate simulations for the last millenium (upper panel), global temperature response in the simulations starting in 1000 A.D. and 1500 A.D. (middle panel) and 100-year running temperature trends (lower panel).*

For the climate simulations covering the last 7000 BP of the Holocene (Oetzi) the following variations in the orbital forcings are also relevant:

- the change in the timing (precession) of the closest point of the Earth to the sun (perihelion), relative to the equinoxes , with a period of ca. 19000 years,
- the angle made by the earth's axis and the orbital plane (obliquity of the ecliptic) with a period of ca. 40000 years and
- the eccentricity as an important parameter of the orbit that defines, as an elipse, its deviation from a perfect, with a period ca 100000 years.

These orbital forcings, which modulate the insolation received by the Earth's at different latitudes and calender month, can be accurately calculated, whereas the other forcings (changes in the solar constant and greenhouse gases) depend on estimations from proxy data.

Fig. 5 gives an overview about the relevant external forcings for the simulation of the last 7 k BP years.

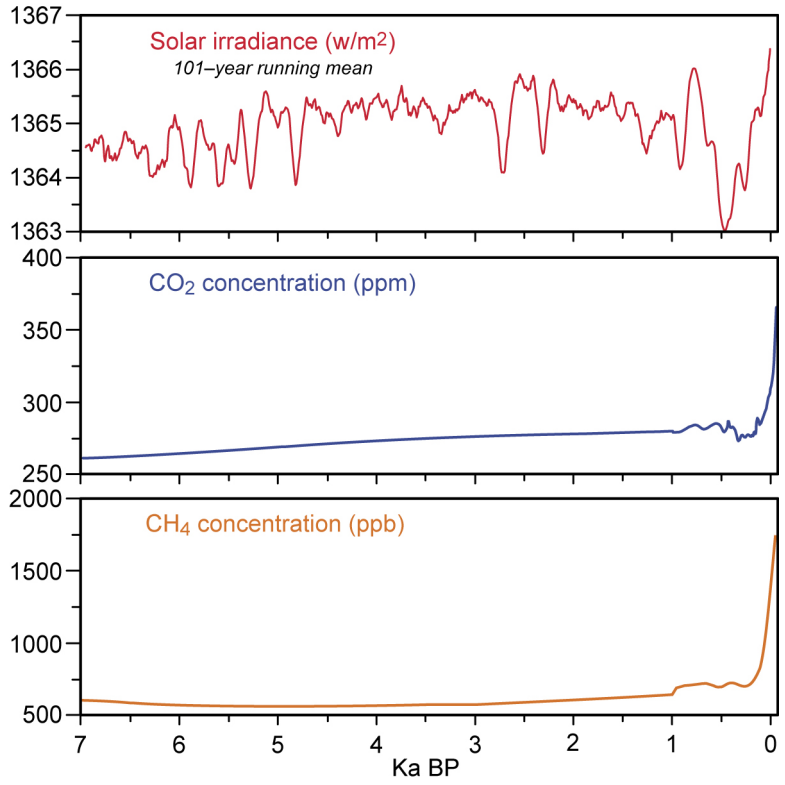

Fig. 5: *External forcings for the Oetzi 2 simulations: upper panel, solar irradiance; middle panel; atmospheric concentration of CO2; lower panel; atmospheric concentration of CH4.*

For the climate simulations with ECHO-G, the CO_2 and NH_4 concentrations are taken from concentration from air bubbles trapped in polar ice-cores (Etheridge et al. 1996, Flückiger et al. 2002). Due to the high uncertainty involved in the reconstruction of the volcanic activity during the time of the mid-Holocene, this forcing was not included in the Holocene simulations (Oetzi).

The intrinsic solar irradiance, defined as the amount of radiant energy emitted by the sun over

all wavelengths that fall each second on 1m² outside Earth's atmosphere caused by internal solar dynamics, is derived from concentrations of the isotopes C_{14} and Be_{10} in ice-cores and after 1610 from historical observations of sunspots (cf. Solanki et al. 2004, Crowley 2000). Produced mainly by cosmic rays, their production rate is modulated by the solar open magnetic field, which is assumed to be related to the total irradiance.

Two simulations have been carried out covering the past millennium, denoted as Erik 1 and Erik 2 (see Fig. 2). Both simulations were driven by the same external forcing, and they only differ in the initial conditions, which were warmer in Erik 1. Since the initial conditions at year 1000 are unknown, both simulations provide a range of the possible climate trajectories under the same external forcing. For more details about the experimental setup of the millennium simulations see von Storch et al. 2004 and Zorita et al. 2004.

For the Holocene climate simulations, the first experiment (Oetzi 1) has been carried out using only variations in the orbital forcings between 7 ka BP and 4.5 ka BP (Berger and Loutre 1991) and solar irradiance and greenhouse gases were kept constant. Fig. 6 shows the differences between time periods of the mid Holocene (7, 6 and 5 ka BP) and the present-day values due to orbital forcing.

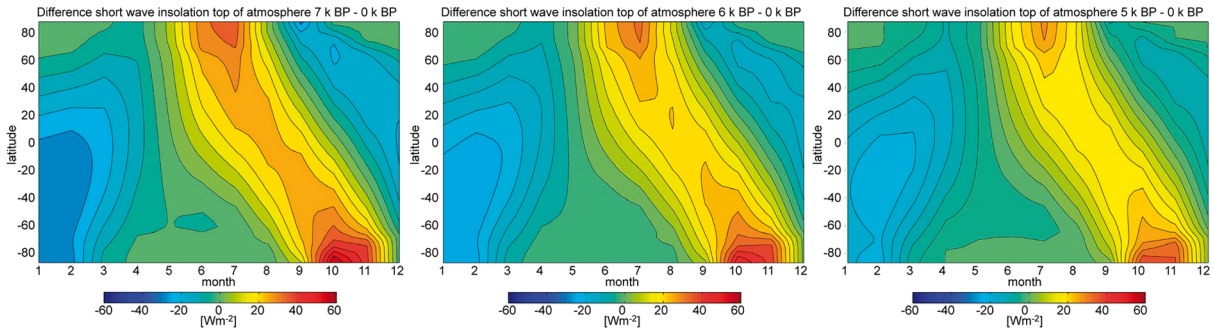

Fig. 6: *Insolation difference between different time periods of the mid-Holocene (7, 6 and 5 ka BP) and present-day caused by changes in orbital parameters (adapted from Wagner et al. 2007).*

In the Northern Hemisphere the insolation anomaly is positive during summer (June-July-August) and negative during winter (December-January-February). In the course of the mid-Holocene the amplitude of the insolation differences decreases which leads to a decrease in

the seasonality.

The second experiment (Oetzi 2) has been carried out using, additionally, solar and greenhouse gas forcing. The solar forcing was estimated by scaling production estimates of Δ14C (cf. Solanki et al. 2004) such that the difference between present-day and Maunder Minimum solar activity is 0.3%. Fig. 7 shows the solar irradiance at top-of-atmosphere for the period 7000 to 4500 BP.

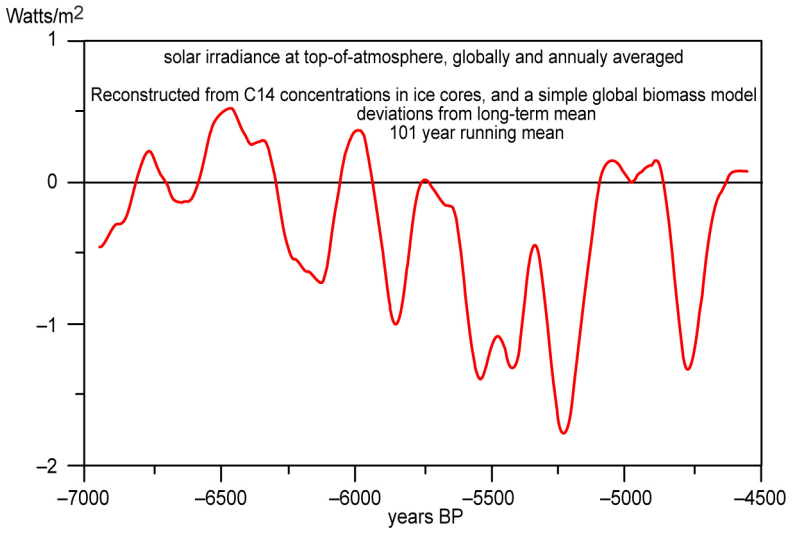

Fig. 7: *Solar irradiance, taken and re-scaled from Weber and Crowley (2004).*

More details about the set up of the climate simulation can be found in Wagner et al. 2007.

2.2.3.3 Climate model scenarios

As stated before, one millennium simulation (Erik 1) was extended until year 2100 AD under the IPCC SRES future scenarios of greenhouse gas concentration A2 and B2. For the study of the contribution of regional climate drivers to future sea-level changes, these scenarios runs were regionalised (together with climate simulations with the GCMs HadCM3 and ECHAM4/OPYC3) by statistically downscaling within the project phase SINCOS I (Hünicke and Zorita 2007). During SINCOS II (2007-2009) this analysis was continued (and updated)

by the application of the statistical downscaling approach to the output of different climate model simulations driven by fourth IPCC SRES 21st century future scenario A2 of greenhouse gas concentrations. Table 1 lists the used five global climate models, along with a reference for more complete documentation. The data, which belongs to the World Climate Research Centre (WCRP) Coupled Model Intercomparison Project (CMIP3) multi-model dataset, were downloaded from the multi-model dataset archive of the Programme of Climate model diagnosis and intercomparison (PCMDI) (http://www-pcmdi.llnl.gov/).

Table 1: *List of Global Climate Models. Additional information on the models and assumed forcings is available at http://www-pcmdi.llnl.gov/ipcc/model_documentation/ipcc_model_documentation.htm (from Hünicke 2009).*

Model	Institution/ Country	Time period	Reference
NCAR CCSM 3.0 (POP OGCM)	National Center for Atmospheric Research/ USA	1870-2099	Meehl et al. 2006
NASA GISS Model E-R (Russell OGCM)	Goddard Institute for Space Studies/ USA	1880-2100	Hansen et al. 2002
UKMO HadCM3	United Kingdom Meteorological Office, Hadley Centre/ UK	1860-2099	Pope et al. 2000
MPI ECHAM5	Max Planck Institute for Meteorology, Germany	1860-2099	Jungclaus et al. 2006
NOAA GFDL CM 2.1	Geophysical Fluid Dynamics Laboratory/ USA	1861-2100	Delworth et al. 2006

In case that a multi simulation ensemble with one model is available, the first simulation, as defined in the dataset archive, is chosen. All models contain forcing by greenhouse gases and tropospheric sulphate aerosols. For more details see Meehl et al. (2007) and Hünicke (2009).

The GCM data grid output was interpolated to the grid resolution of the observational data sets and the geographical window corresponds to the observational climate data sets (see Section 2.2.1).

3 The observational period - Research Focus I

Baltic Sea level records show large trends due to the isostatic post-glacial rebound. Is it possible to identify the underlying influence of regional climate factors by analysing the amplitude of the annual cycle of sea-level, which is not affected by the isostasy?

3.1 Establishment of statistical approaches in the observational record

One of the difficulties to identify the influence of climate factors on Baltic Sea level is the presence of the strong isostatic sea-level trend. The transfer function linking sea-level records with regional climate variables have been developed and tested within SINCOS I by a statistical downscaling approach based on regression analyses (transfer functions). This approach was dependent on the isostatic trend contained in the sea-level records (Strategy I). To learn more of the robustness of these results, we applied within SINCOS II another statistical approach, which is independent of the isostatic trend contained in the sea-level records by analysing monthly differences in the amplitude of the mean annual cycle in Baltic Sea level by trend analyses (Strategy II).

In the following, a recapitulation of Strategy I (Statistical Downscaling) and a more detailed view on Strategy II (Trend Analysis) will be presented. The application of the statistical downscaling approach to the output of global climate simulations will be explained more precisely in Section 4.3.

3.1.1 Statistical Downscaling

The method is based on linear regression models, which establish a statistical relationship between Sea level as predictand (regional scale dependent variable) and large scale climate fields as predictors (independent variables). For the calibration and validation of the regression models, different time periods within 1800 to 2000 are tested (e.g. calibration period 1951-1998, validation period 1900-1950) examining the skill of different predictors.

The predictors were restricted to those that are potentially well simulated by coarse resolution models (GCMs).

At decadal timescales and at mid-latitudes, surface wind is closely related to SLP through the geostrophic relation. Furthermore, SLP gradients may also influence sea-level through the inverse barometric effect. SLP is therefore considered as the first predictor in a simple regression equation with sea-level at one station SL_i as the predictand. The SLP field in the European region is previously decomposed in its principal components (PCs) to avoid co-linearity of the predictors and the resulting instability of the regression which simplified reads

$$SL(t) = \sum_{i=1,N} a_i \, pc_i \,(t) + SLR \;\; (t)$$

where pc_i is the i^{th} PC, a_i is the corresponding regression coefficient, N the number of PCs included in the regression and SLR are the sea-level residuals. The parameters a_i were calibrated in the corresponding period (e.g. 1950-1999) by least-square error minimization. To estimate sea-level variations outside the calibration, the SLP anomalies relative to the calibration period are projected onto the Empirical Orthogonal Function (EOF) previously calculated in the calibration period. The number N of PCs included in the regression was the one yielding the best model skill in the validation period. In further steps the statistical model has been augmented to include winter precipitation and winter air-temperature as a sole predictor, with both representations (Baltic Sea area averaged and PCs) and also the predictor skill of temperature in combination with SLP has been tested.

The results indicated that the influence of different large-scale forcing factors on sea-level vary geographically. While the decadal sea-level variations in the northern and eastern Baltic gauges are strongly influenced by the atmospheric circulation, decadal variations in the Southern Baltic Sea can be (statistically) better explained by area-averaged precipitation. The effect of temperature variations is either already contained in the SLP field or is less important for decadal sea-level variations than the other two factors (see Hünicke and Zorita 2006; Hünicke et al. 2008).

1.2 Trend Analysis

Although the influence of isostasy on sea-level cannot be statistically separated from long-term trends in climate factors that may also be influencing sea-level, it is reasonable to assume that the trend *difference* between any two seasons of the year has to be related to factors different from isostasy. For instance, the trend in the sea-level difference between winter and the following early spring, i.e., the trend in the amplitude of the annual cycle, is very probably unrelated to isostasy, as the influence of isostasy at time-scales of a few months is negligible. This fact is exploited to identify the influence of long-term climate forcings on Baltic Sea level.

For the 19th and 20th century, Hünicke and Zorita (2008) found that Baltic Sea level shows a mean annual cycle with a minimum in early spring and a maximum in winter. The amplitude of this annual cycle (maximum minus minimum) ranges between values of 10 to 30 cm and shows an increase of around ~0.8mm/year in the 20th century in almost all gauge stations analysed (Fig. 8).

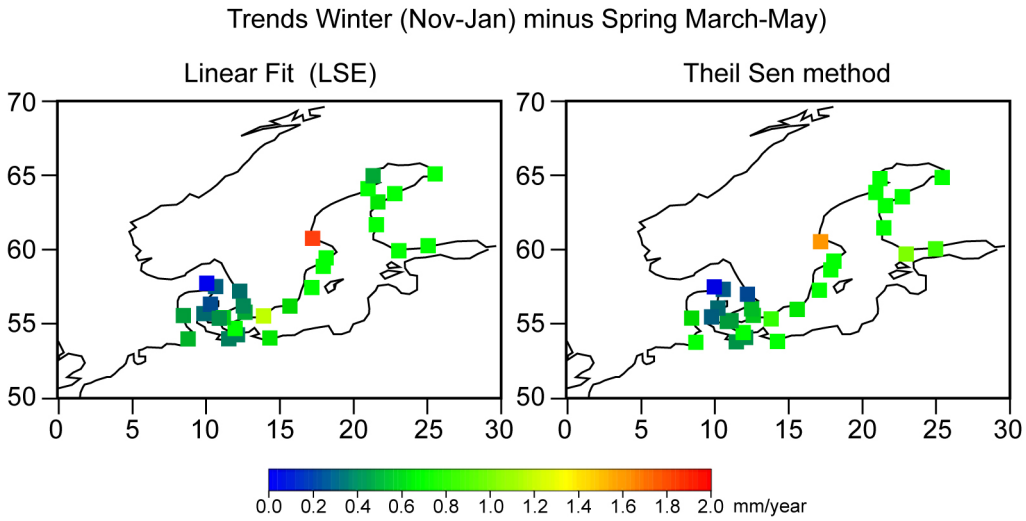

Fig. 8: *Trends in the amplitude of the sea-level annual cycle winter minus spring in the Baltic Sea estimated in the 20th century by a least-square-error linear fit and by the non-parametric Theil-Sen method (from Hünicke and Zorita 2008).*

These trends are not large compared to the decadal variations of the annual cycle, but they are statistically significant. The magnitude of the trends is almost spatially uniform, with exception of the Skagerrak area. Since inter-annual and decadal variability of sea-level displays a clear spatial pattern, the mechanism responsible for the trends in the annual cycle seem to be not regional, but affect the Baltic Sea basin as a whole.

The question arises about which factor - or factors- are responsible for the long-term trend in the amplitude of the annual cycle. To answer this question, several hypotheses are proposed as mechanism to explain the centennial trends in the winter-minus-spring sea level: the effect of wind (through the SLP field), the barometric effect, temperature and precipitation (including role of salinity).

The strength of westerly winds, which strongly influence sea-level variations and its northern and eastern boundaries in wintertime at inter-annual timescales, is closely related to the North Atlantic Oscillation (NAO). In general, a positive trend in the NAO-index in winter would lead to a positive trend in winter sea-level and therefore could explain the more positive trend in wintertime relative to spring. It is found that the winter NAO-index shows a negative trend in the 20th century for the months November-January with a mean decrease in 100 years of roughly one half of the inter-annual standard deviation. However, the NAO, as the dominant SLP large scale pattern, explains on average only 32% of the total variability of sea-level at inter-annual timescales (Kauker and Meier 2003). Thus, the remaining SLP variability pattern should also be taken into account. One possible method to do so is to perform a regression analysis linking sea level variations as predictand and sea-level pressure as predictor and analyse the trend which is detectable in the reconstructed sea-level, out of the regression, which is caused by the SLP-field. Again, a negative trend for all station is found.

In a next step the sign of barotropic trends was investigated, calculating the pressure differences between the Baltic Sea Region (10E to 30E and 50N to 65N) and the North Atlantic Area (30W to 10E and 50N to 65N). Indeed, the difference of the winter and spring barometric gradients was found to produce a difference between winter and spring sea-level of the order of +0.15 mm/year, but the barometric effect is too small to explain these trends.

Might increasing temperature, due to the thermal expansion of the water column, be a plausible factor to explain the centennial increasing trend in the amplitude of the annual cycle

of Baltic Sea level? Fig. 9 shows the evolution of the average air-temperature in the Baltic-Sea region smoothed by an 11-year running mean filter for the winter and spring seasons for the 20th century.

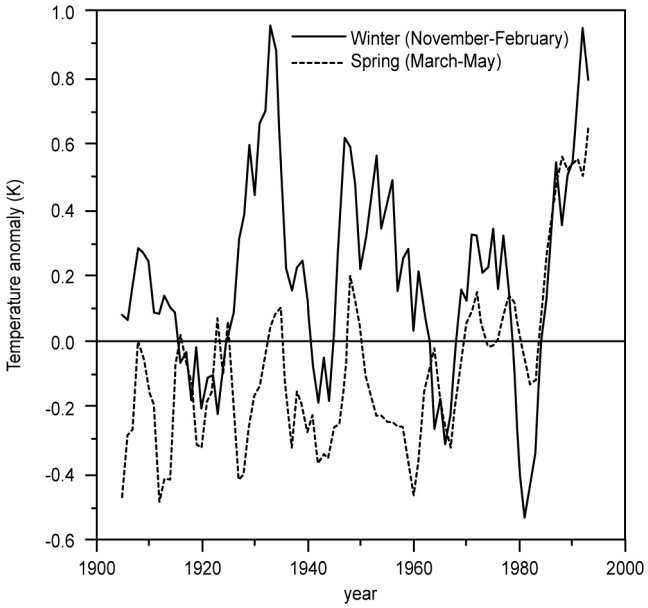

Fig. 9: *Decadally smoothed winter (solid line) and spring (dashed line) averaged air-temperature in the Baltic Sea region in the 20th century (from Hünicke and Zorita 2008).*

A positive trend in winter and spring could be detected, but which larger centennial trend values in spring. Taking into account a possible penetration depth of temperature (winter 100m, spring 20m), the effect on sea-level is found to be too small.

Hünicke and Zorita (2006) and Hünicke et al. (2008) found precipitation to explain a part of the decadal variability of Baltic sea-level variations in summertime in the 20th century. According to that analysis, higher than normal precipitation is linked to higher than normal sea level in summertime, but they did not analyse precipitation trends in other seasons, e.g. trends in the spring precipitation. However, if this link is also present in spring and maintained at centennial time-scales, a negative trend in spring precipitation could explain a more positive sea-level trend in winter with respect to spring, thus contributing to the explanation of the widening winter-minus-spring sea-level difference.

Fig. 10 depicts the spatially averaged spring and winter precipitation time-series, smoothed with an 11-year running mean, for the period 1900 to 1996.

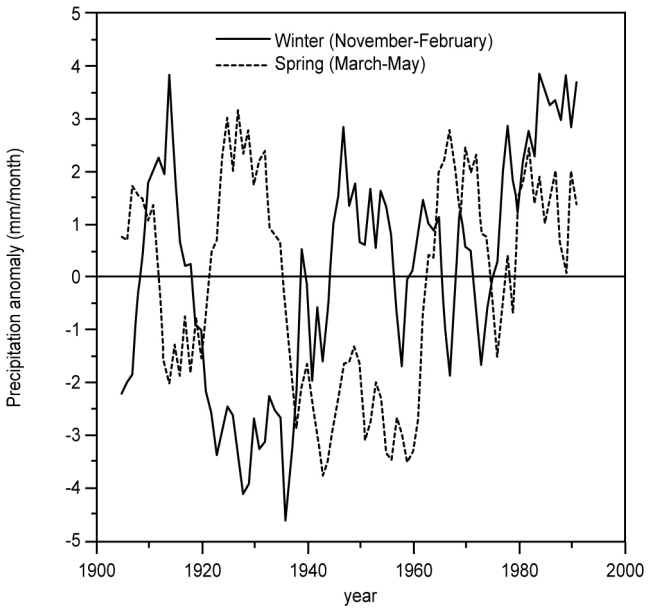

Fig. 10: *Decadally smoothed winter (solid line) and spring (dashed line) averaged precipitation in the Baltic Sea region in the 20th century (from Hünicke and Zorita 2008).*

It can be seen that spring precipitation in the Baltic Sea shows indeed a slight positive trend in the 20th century (1.4 ±4 mm/month per century, 95% confidence interval), whereas in the winter months the trend is also positive but much larger (5 ±4 mm/month per century). Thus, the trend in winter precipitation is statistically significant whereas spring precipitation can be considered as trendless in practical terms. The difference in trends in winter and spring precipitation could in principle explain the increasing difference between winter and spring sea-level observed in the last 100 years.

Of all explanations tested, the long-term trend in seasonal Baltic precipitation seems to be the most plausible candidate for the increasing amplitude of the annual cycle. For the other three either the sign or the magnitude of the trend make them problematic to be included as a sole explanation. These results, obtained by Strategy II (Trend Analysis) support the findings based on Strategy I (Statistical Downscaling).

4 Climate model simulations - Research Focus II

What can we learn from climate model simulations of Baltic Sea-level variations over the past decades to millennia's for future times?

4.1 Global climate model simulations and the Baltic Sea

Present global climate models (GCMs) have a horizontal spatial resolution in the range of 2 to 4 geographical degrees. Due to the coarse spatial resolution, the Baltic Sea is only very schematically represented in current GCMs by a few grid cells. Fig. 11 shows the land-sea mask of the ECHO-G model for the Atlantic-European Sector together with the atmospheric grid for the Baltic Sea Region.

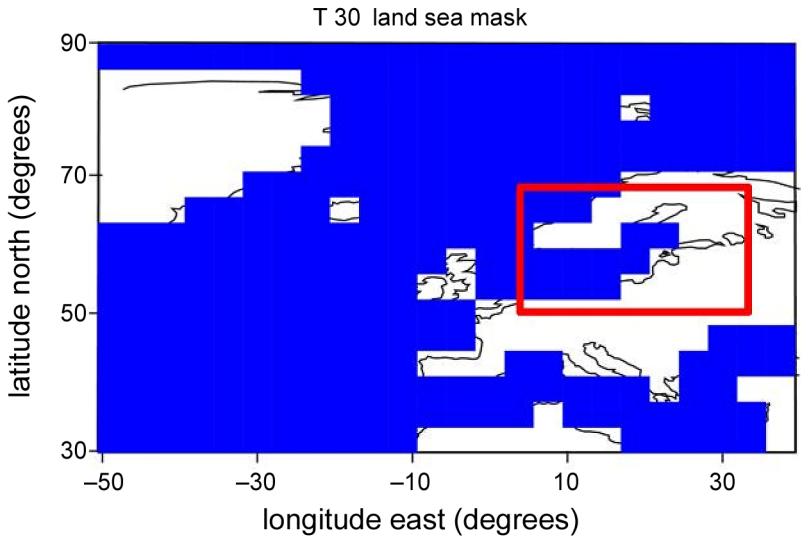

Fig. 11: *The ECHO-G land-sea mask for the Atlantic-European sector. The Baltic Sea Region is indicated by the red square.*

Here, the horizontal resolution of ca. T30 reflects grid cells of ca. 200 km longitude and 400 km latitude. Thus, important topography-depended processes, like the exchange of water masses between the North Sea and the Baltic Sea, the large heterogeneity in precipitation (due

to the presence of mountain ranges in the Scandinavian Peninsula) or the basins of the Baltic Sea (and the exchange of water masses between them) cannot be properly accounted for. To regionalise the information in the large scale forcing fields provided by the GCMs, the application of downscaling methods is required (see Section 3.1.1).

4.1.1 Evaluation of the model skill of ECHO-G

For the last millennium, ECHO-G shows, globally, a good skill in simulating the seasonal mean climatology and interannual variability of SLP, near-surface temperature and precipitation. The simulated Northern Hemisphere (NH) wintertime spatial SLP patterns, in particular the North Atlantic Oscillation (NAO) and their variability was found to agree well with observations (e.g. Min et al. 2005b, Raible et al. 2005, Gouriand et al. 2006).

The Holocene climate simulations for the period 7-0 ka BP have been finished recently. Thus, no peer-reviewed studies for comparison and evaluation of the results for our region of interest exist yet. Also, no other long climate simulations of this kind exist yet, which gives the simulations performed at GKSS, up-to-date (2009) a unique status. The analysis of these simulations for different focus regions of the world is in ongoing work and the results are planned to be published soon.

However, the realism of these long climate simulations in the Baltic Sea sector can be ascertain by comparing certain key variables, such as air-temperature, with adequate reconstructions based on proxy data. See Chapter 5 for more details.

4.2 Results

Here, the main results of the simulated climate in the Baltic Sea Area for the last millennium (as a recapitulation) and the Holocene period 7k BP to present (as the key focus of SINCOS II) will be briefly presented. As the simulated wind is of major interest for the morphodynamic paleo-modelling within SINCOS II (e.g. Zhang et al. 2009; Meyer et al. 2009), it will be also briefly presented and discussed.

As stated before, the resolution of ECHO-G is too coarse to reasonably resolve the Baltic Sea. The output of the climate simulations cannot, therefore, be interpreted at small regional scales without a regionalization. However, the simulated climate variables allow for a rough estimation of the internal variability at multidecadal and regional timescales, as they differ only in their initial conditions.

Thus, in the following the emphasis will be put on larger-scale climate patterns of relevance for the Baltic Sea region. A regionalization due to downscaling techniques will be presented later on in Section 4.3.

Note that the climate model output refers to calendar years before present (cal BP=1950) and are not equivalent to the conventional C_{14} age dating. This has to be considered careful by comparing the climate simulation results to the results out of radio carbon dating proxy data and others. For more information see Stuiver et al. (1998).

Fig. 12 shows the atmospheric grid of the ECHO-G model for the Baltic Sea Area.

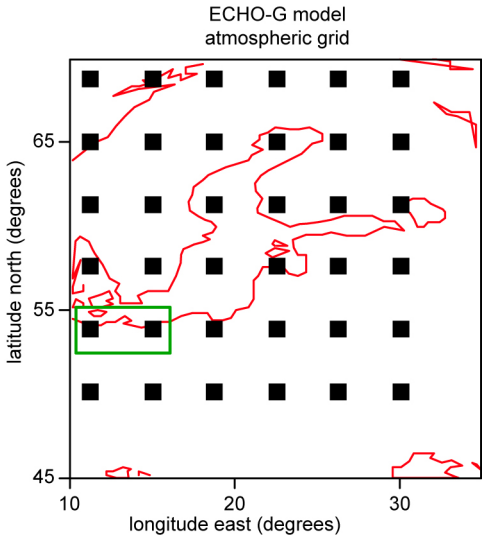

Fig. 12: *Atmospheric grid of the ECHO-G model for the Baltic Sea Area with 36 cells (ca. 6°x6° degrees) in the geographical box 11,25E-30E, 49, 75N-68,5N. The green square indicates the two grid points, which are used for the analysis of the wind time series for the South-western Baltic Coast.*

The results presented in the following are, in general, based on the mean of this 36 grid cells.

4.2.1 Some Results for the simulation Erik

4.2.1.1 Temperature

For the Baltic area annual mean temperature, the two twin simulations show a general centennial agreement, but also deviations at multi-decadal timescales (Fig. 13, left panel). This means that the comparison between model simulations and proxy records has to take into account that the internal variability at multi-decadal timescales is not negligible, and therefore an agreement between models and proxy data at these temporal scales is not compulsory.

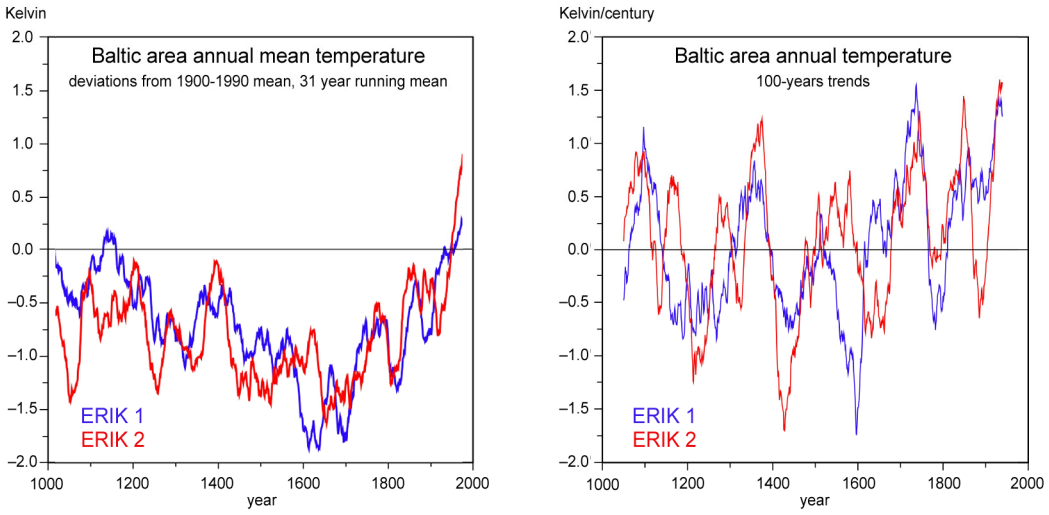

Fig. 13: *Simulated Baltic Sea near surface annual temperature taken from the ECHO-G millennium simulations Erik 1 and Erik 2. Left panel: deviations from 1900-1990, smoothed by a 31- year low-pass-filter. Right panel: 100 year linear trends.*

The recent (up to 1990) warming rate is not unprecedented (Fig. 13, right panel). This warming rate is larger across simulations temperature variability in winter (ca. 1.5 K per century) than in summer (0.75K per century) (see Fig. 14 and Fig. 15). The long-term warming trend in the past few centuries agrees in all four simulations. This indicates that the internal random variations at these long time scales are very small in the model. If this is also the case in reality, proxy records and model simulations at multi centennial time scales should agree. A disagreement would be indicative of deficient simulations or errors in the proxy records.

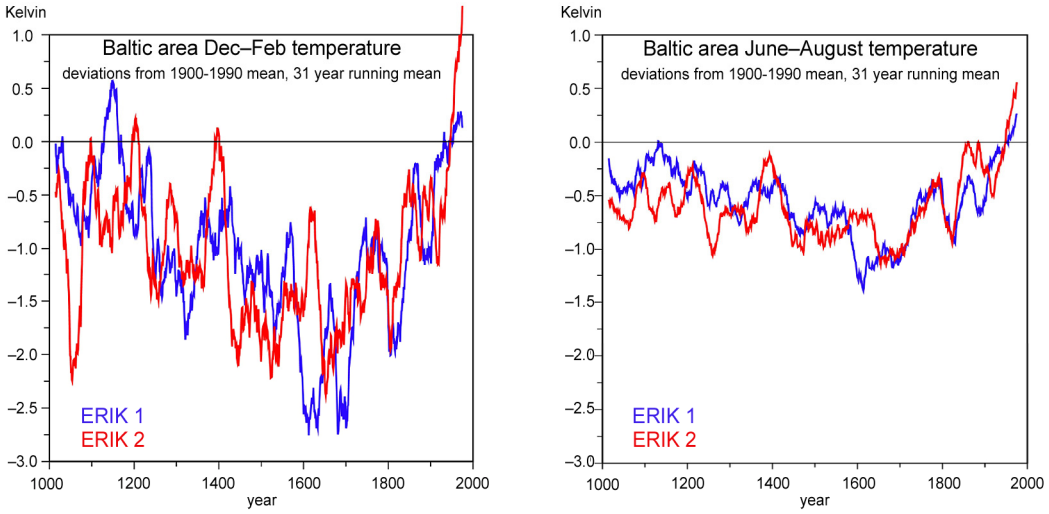

Fig. 14: *Simulated Baltic Sea seasonal near-surface temperature means taken from the ECHO-G millennium simulations Erik 1 and Erik 2. Deviations from 1900-1990, smoothed by an 31- year low-pass-filter. Left panel: winter mean (December-January-February). Right panel: summer mean (June-July-August).*

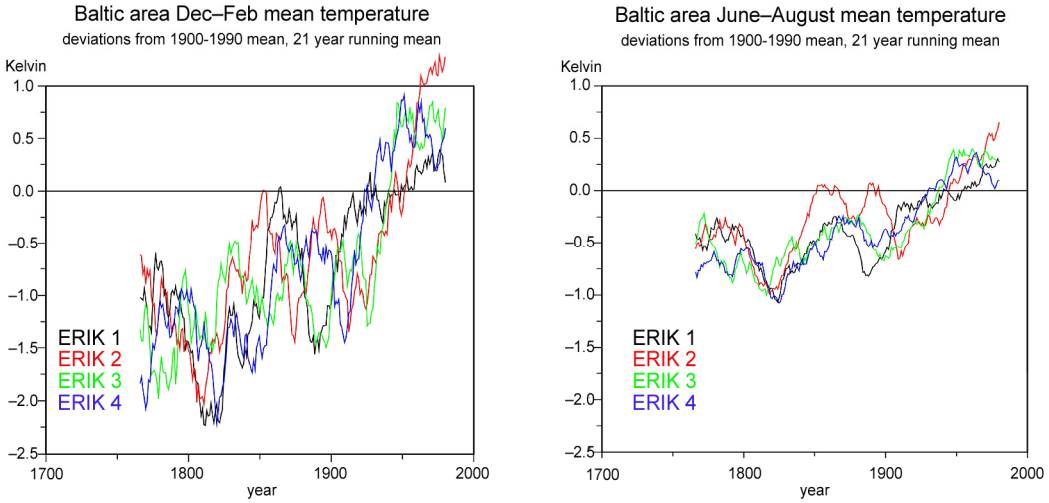

Fig. 15: *Simulated Baltic Sea seasonal near surface temperature means for the millennium simulations Erik 1-4, deviations from 1900-1990, smoothed by a 21- year low-pass-filter. Left panel: winter mean (December-January-February). Right panel: summer mean (June-July-August).*

4.2.1.2 Precipitation

For the Baltic area annual mean precipitation, the two twin simulations show a small across simulation variability (Fig. 16, left panel). The recent precipitation trends in the 20th century (Fig. 16, right panel) are not unprecedented and reasonable agree with observations with trend values of ca. 4 mm/ month/century. They are tightly coupled to external forcings.

To conclude, at multi-decadal scales, the regional variability may be just internally generated and model simulations and proxy-based reconstructions do not have to agree, but at centennial scales, the regional variability is due to the forcing. For more information see Zorita et al. 2007.

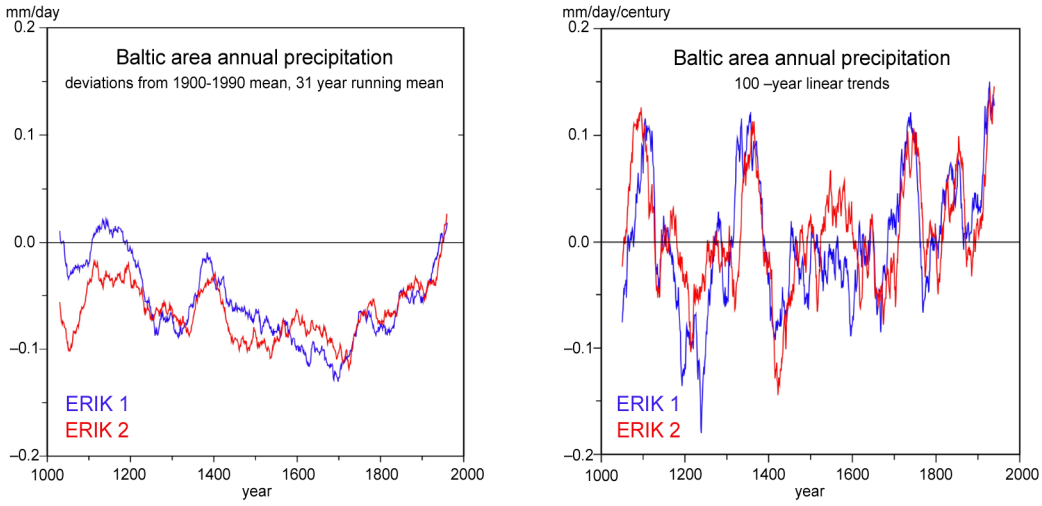

Fig. 16: *Simulated Baltic Sea annual mean precipitation for the millennium simulations Erik 1 and Erik 2. Left panel: deviations from 1900-1990, smoothed by a 31-year low-pass-filter. Right panel: 100 year linear trends.*

4.2.1.3 North Atlantic Oscillation

The analysis of the Erik simulations with regard to the stability of the NAO-influence on the regional climate of the Baltic Sea Area indicates that this relationship may vary in time. However, this variations are not related to the external forcing, i.e. it is nor larger or smaller in periods with generally warmer or colder temperatures (Schenk et al. 2009). This leads to the conclusion that the non-stationarity in the relationship between the NAO and the regional

climate is mainly the result of internal climate variability. However, the question arises if the external forcing factors might have an influence on longer time scales due to orbital change (see Section 4.2.2).

4.2.1.4 Wind

Fig. 17 gives information about the spatial heterogeneity of the simulated 10m-wind time-series (annual and seasonally) over the selected Baltic Sea Grid.

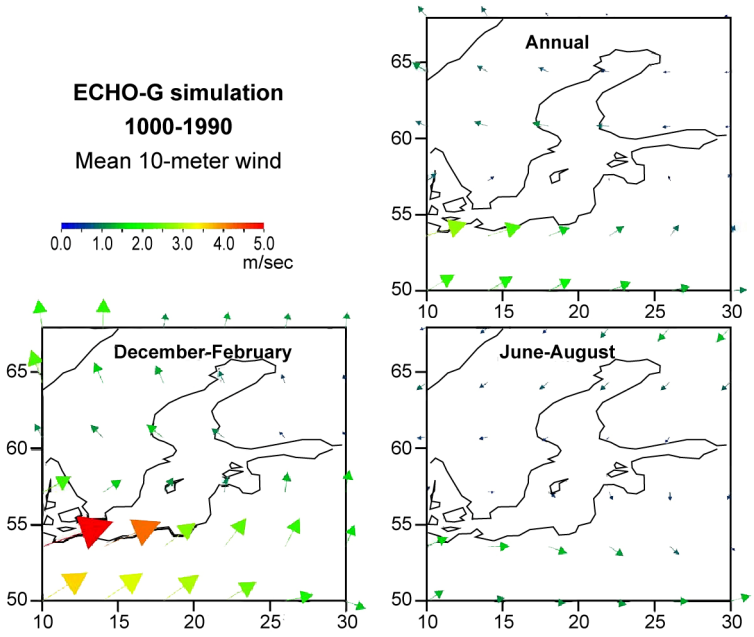

Fig. 17: *Simulated Baltic Sea mean 10m-winds taken from the millennium simulation Erik 2, averaged over the simulated time period (1000-1990) for each of the 36 Baltic Sea grid points, respectively (Fig. 12). Upper panel: annual means. Lower panels: seasonal means for winter (left) and summer (right).*

The analysis shows spatial differences for the main wind directions between the southern and northern parts of the Baltic Sea. While in the Southern part the main simulated wind direction is SW, in the northern parts the wind direction various around NE /NW with much lower values. In winter, this spatial pattern is, as expected, even more pronounced with much higher values in SW wind speed (up to 4-5 m/sec) in the Southern parts of the Baltic Sea. The

question arises as to how close these model results are to reality? To answer this question, the simulated model results were compared to 'observed' data taken from Reanalyses Data[3] (Fig. 18).

Although this reanalysis (observational) dataset only covers a time period of 50 years (1948 - 2005), the values of Fig. 18 and Fig. 17 allow for a rough comparison, as they present mean values over time.

In general, in the model simulations the wind speed appears, on average, weaker than in the observations, especially in the north. The wind directions in areas with high wind speeds are in the mean realistic, but overestimated in the model simulation (especially for the Southern Baltic Coast in winter). This under- and overestimation in the wind-speed seems season-depended. This was also found by a more detailed analysis of these datasets by Zhang (personal comment 2009).

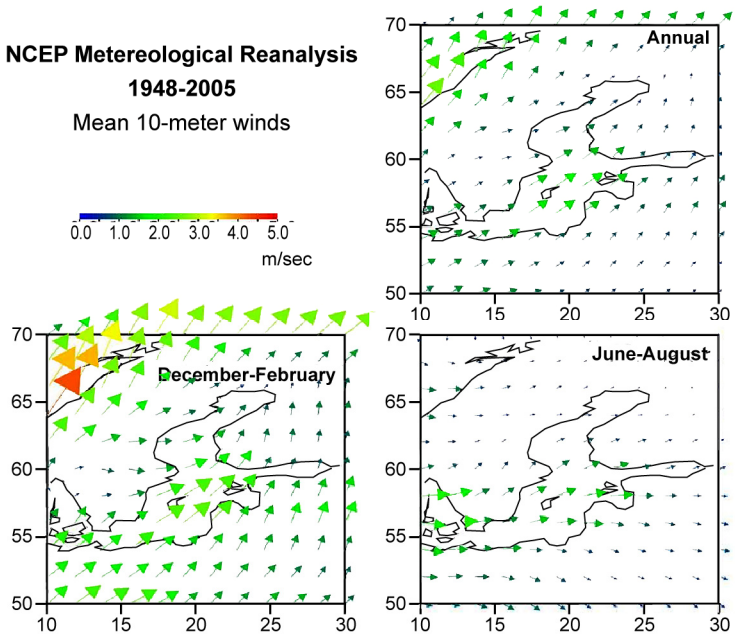

Fig. 18: *Baltic Area mean 10m-winds taken from the NCEP Meteorological Reanalysis, averaged over the time period 1948-2005 for each of the 36 Baltic Sea grid points, respectively (Fig. 12). Upper panel: annual means. Lower panels: seasonal means for winter (left) and summer (right).*

3 Result of homogenous data assimilations with a weather prediction model in hindcast modus.

4.2.1.5 Other Erik studies

Several other recent published research studies focused on the millennium climate simulations (Erik) performed at GKSS. In the following, the outcome of two of them –related to the SINCOS research –shall be summarised in brief.

In collaboration with the Stockholm University (Sweden) the climate variability in Scandinavia for the past millennium was studied by GKSS ECHO-G simulations (Erik). The analysis showed that the model simulate quite realistically the observed relationships between the atmospheric circulation and temperatures in Scandinavia for summer and winter. Especially in winter, the simulated relationships appear to be in good agreement with instrumental observations on longer and shorter timescales and the simulated long-term temperature evolution agrees broadly with proxy data. For more details about this work see Gouirand et al. 2007.

In collaboration with the University of Madrid (Spain) the relationship between global mean sea-level and global mean temperature in the Erik simulations has been studied for the past millennium. Thereby, it was explored if it is possible to use the global mean near surface temperature, its rate of change or the global mean ocean heat-flux as predictors to statistically estimate the change of global mean sea-level. It could be pointed out that a simple linear relationship between the mean temperature and the rate of change of sea level does not exist. The ocean heat-flux and the rate of change of mean temperature seem to better capture the rate of change of sea level due to thermal expansion. For details of this study see von Storch et al. (2008).

4.2.2 Results for the simulation Oetzi

4.2.2.1 Temperature

Fig. 19 shows the simulated Baltic Sea area near-surface temperature, annual and seasonally, for both model experiments taking only variations in orbital forcing (Oetzi 1) and variations in orbital forcing, solar irradiance and greenhouse gases (Oetzi 2) into account (see Section 2.2.3.2 for more details).

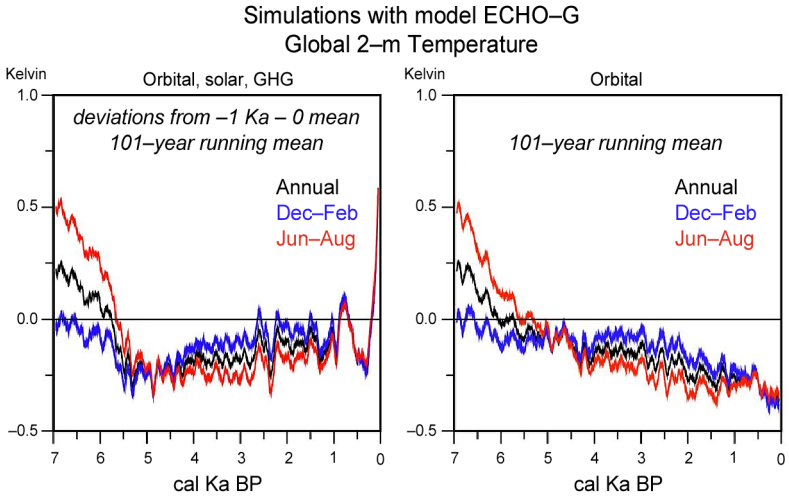

Fig. 19: *Simulated Baltic Sea seasonal near-surface temperature means taken from the ECHO-G Holocene simulations Oetzi 1 (right panel) and Oetzi 2 (left panel). Deviations from -1 Ka -0 mean, smoothed by a 101- year low-pass-filter. Annual (black), winter (blue) and summer (red) mean.*

At first view, a natural cooling trend can be identified for both model simulations which points to the assumption that the orbital parameters are responsible for this trend. However, around the Holocene Optimum (around 6000BP) the time-series show deviations and the second experiment (including solar and greenhouse gas forcing additionally to the orbital forcing) seems to generate a warm mid-Holocene more clearly than the first experiment (including just orbital forcing). Also, a jump in the trend around 5500BP is visible, which has to be analysed in more detail.

The seasonal (winter and summer) simulated temperature anomalies (Fig. 19, blue and red graphs) show, in general, a good agreement with a Holocene temperature reconstruction for the North East (NE) Region from Davis et al. (2003) with a distinctly increased annual mean mid-Holocene (around 6 ka BP) temperature in comparison to pre-industrial climate.

This result was also found by Otto et al. (2009) who analysed simulations with a coupled atmosphere-ocean-vegetation GCM in terms of feedback separation and synergies for the mid-Holocene climate.

Also, a clear decreasing trend in summer temperature until 7000 cal BP can be detected in

both –the proxy data (Davis et al. 2003) and the simulated time-series (ECHO-G).

For an interesting application of these findings see also Schmölcke (2008), who studied the Holocene environmental changes in the seal (Phocidae) fauna of the Baltic Sea (within SINCOS II).

4.2.2.2 Precipitation

Fig. 20 shows the time series for the simulated annual and seasonal (winter and summer) Baltic area precipitation for the model experiment, taking variations in orbital forcing, solar irradiance and greenhouse gases (Oetzi 2) into account.

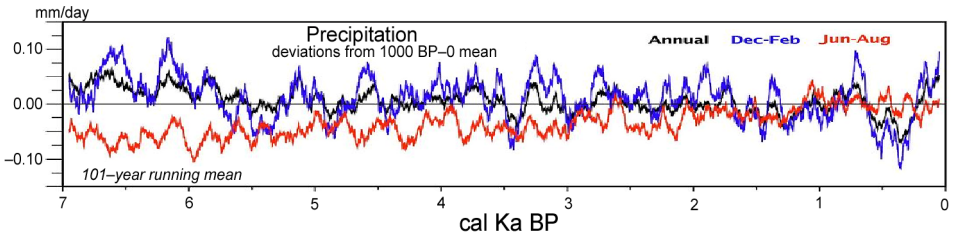

Fig. 20: *Simulated Baltic Sea near-surface temperature means taken from the ECHO-G Holocene simulation Oetzi 2. Deviations from -1 Ka -0 mean, smoothed by a 101- year low-pass-filter. Annual (black), winter (blue) and summer (red) mean.*

Here, also a decreasing trend can be detected. The explanation behind this is that decreasing temperatures causes a general drying of the atmosphere, which leads to reduced precipitation. Again, a jump in the trend around 5500 cal BP is visible.

4.2.2.3 North Atlantic Oscillation

Fig. 21 shows the simulated NAO-index for the summer and winter season, smoothed by a 101-year running mean.

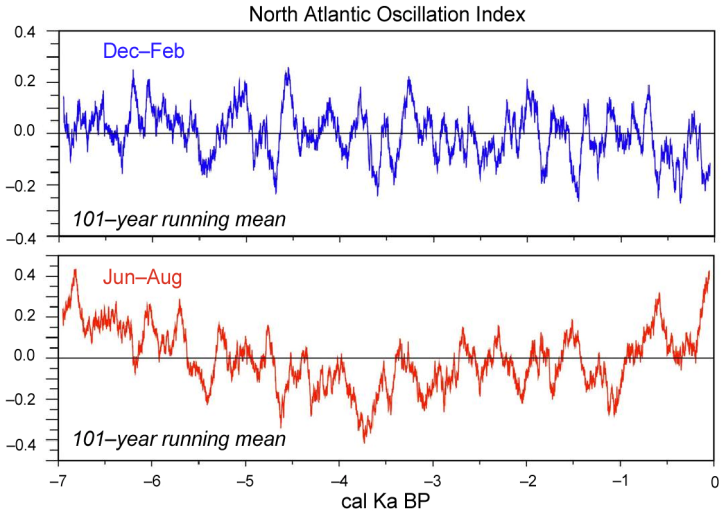

Fig. 21: *Simulated Baltic Sea seasonal NAO-Index taken from the ECHO-G Holocene simulation Oetzi 2. Deviations from -1 Ka -0 mean, smoothed by a 101- year low-pass-filter. Winter (upper panel) and summer (lower panel) mean.*

It seems that the strength of the NAO in wintertime tends to a slightly decrease, which is associated with a long-term decrease in westerly winds. This evolution is not visible in summer. This behaviour is probably related to the temperature meridional gradient across the North Atlantic. However, the comparison of the simulated winter (DJF) NAO indexes of Oetzi 1 and Oetzi 2, shows no long term trend (Fig. 22, 7 k cal BP to 2.5 k cal BP).

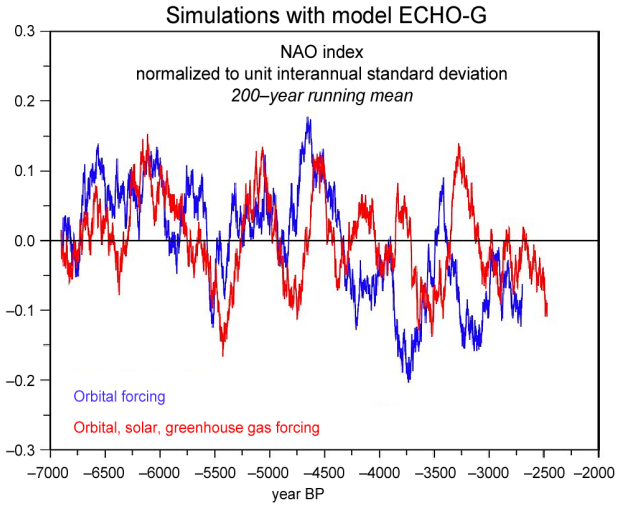

Fig. 22: *Simulated Baltic Sea seasonal NAO-Index taken from the ECHO-G Holocene simulations Oetzi 1 (blue) and Oetzi 2 (red). Deviations from -1 Ka -0 mean, smoothed by a 101- year low-pass-filter.*

This suggests that the variations in the NAO index are not related to the forcings and are of internal nature (as the two time series show different developments).

4.2.2.4 Wind

A specific interest of the simulated wind lies in the application of the long wind time-series to multi-scale centennial-to-millenial morphodynamic modelling approaches performed within SINCOS for the Southwestern Baltic Sea Coast (e.g. Zhang et al. 2009; Meyer et al. 2009).

Fig. 23 shows the simulated Holocene mean 10-m wind for the Southern Baltic Sea region (based on the mean of the two selected grid points, see Fig. 12), annually and seasonally, for the time period 7-0 k cal BP (Oetzi 2) for the west-east and the south-north component.

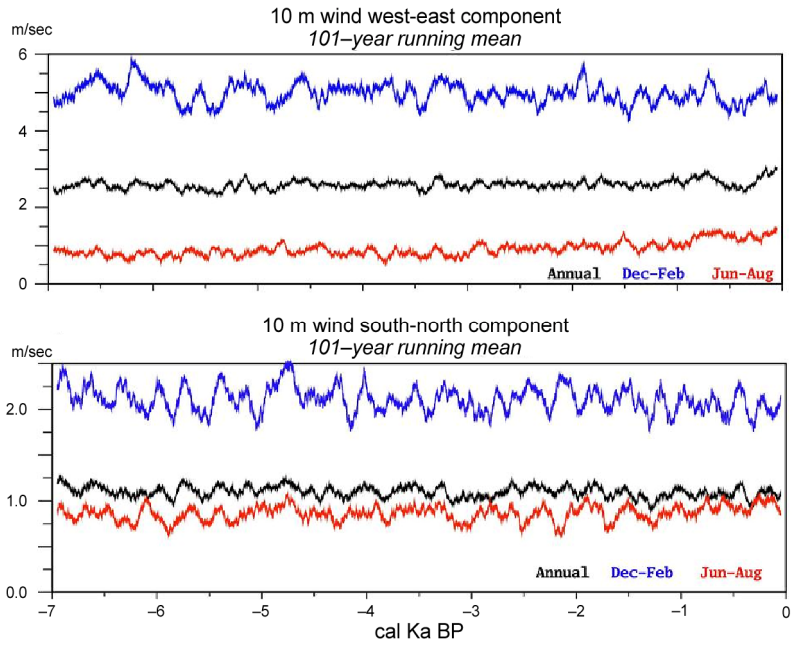

Fig. 23: *Simulated Baltic Sea mean 10m-winds taken from the ECHO-G Holocene simulation Oetzi 2 , based on the mean of the 2 selected grid points for the southwestern Baltic coast (see Fig. 12, green square) Upper panel: west-east component. Lower panel: south-north component. Annual (black), winter (blue) and summer (red) mean, smoothed by a 101- year low-pass-filter.*

The annual (yearly averaged) wind speed shows no long-term trend. Also in the winter (DJF) mean of the 10-m wind, no trend could be detected, whereas the summer (JJA) mean of the simulated wind show a slight increasing trend. The main simulated wind direction comes from South-West (NW).

The mean of the ECHO-G Holocene10m-winds simulation, driven by variations in orbital forcing, solar irradiance and greenhouse gases (Oetzi 2) and averaged over all 36 Baltic Sea grid points, leads to a similar result. However, the simulation results of Oetzi 1 (only orbital forcing) show a slight decreasing trend in the annual and winter mean and no trend in summer.

4.3 Estimation of the contribution of regional climate drivers to winter-sea-level changes in the Baltic Sea

The establishment of statistical relationships between sea level and large scale climate fields in the observational record (Section 3.1) allows an estimation of recent past and future regional climate change by statistical means through the application of the statistical models to the corresponding output of GCM simulations. However, the analysis has to be based on two assumptions: (a) the statistical relationship represents real physical links between the predictors and the sea level, (b) the applied empirical statistical functions that describe the detected influence will remain unchanged in a future climate.

4.3.1 Application of the statistical transfer function to the output of climate model simulations

For the estimation of the contribution of regional climate drivers to past sea-level changes, the statistical downscaling approach is applied to the output of the long Holocene simulations performed with ECHO-G (Oetzi). For the estimation of the contribution to future sea-level changes, the output of different IPCC AR4 coupled GCM simulations driven by SRES A2 future scenarios of greenhouse gas concentrations (see Section 2.2.3.3) is used as predictor. Following Hünicke et al. (2008), the transfer functions are applied to winter means (December-January-February) of four of the longest historical time-series of sea-level records

(up to 200 years) from stations situated in the central, eastern and southern Baltic Coast. For more information read Section 3.1.1 (Statistical Downscaling).

For the central (Stockholm) and eastern (Kronstadt) Baltic Sea level stations, SLP (for the geographical window 30°W to 40°E, 30°-70°N) was used as predictor. Therefore, the SLP field was decomposed to its principal components (PCs) to avoid co-linearity. Once the regression coefficients had been estimated by Least Mean Square-Error, the respective climate model time series associated with the leading SLP PCs were determined for the whole time-period by projecting the simulated SLP anomalies (deviations from the model 1900-1998 mean) onto the observational spatial eigenvectors of loadings from the PC analysis. The regression coefficients were calibrated in 1900-1999 by using gridded climatic data sets of SLP (Trenberth and Paolino 1980) and precipitation (Mitchell and Jones 2005). For the sea-level stations in the Southern Baltic Sea (Swinoujscie and Kolobrzeg) area-averaged precipitation (for the geographical window 11°-26°E and 52°-62°N) was applied as predictor. Thereby, the precipitation time-series is treated the same as a single PC of the SLP field.

4.3.1.1 Contribution of regional climate to past winter sea-level changes

Once the statistical models were validated and physically interpreted, the past sea-level variations related to climatic variations can be reconstructed. The output of the statistical model when driven by simulated fields of SLP and precipitation provides an estimation of the consequences of regional climate variations for Baltic Sea level in the past.

Fig. 24 shows the contribution of the SLP variations simulated in Oetzi 1 and 2 to past winter sea-level changes in two sea level stations in the central and eastern Baltic based on the empirical transfer functions derived from observations.

In both simulations SLP contribute to a slight decreasing trend in sea-level in Stockholm and Kronstadt. This trend is more marked in the simulation with orbital forcing only, which indicates that in this respect the long-term influence of greenhouse gas forcing and solar variations is opposed to the orbital forcing. Since the SLP is affected more by the spatial temperature gradients than by the temperature itself, it is not straight forward to disentangle

the physical mechanisms that bring about these long-term trends.

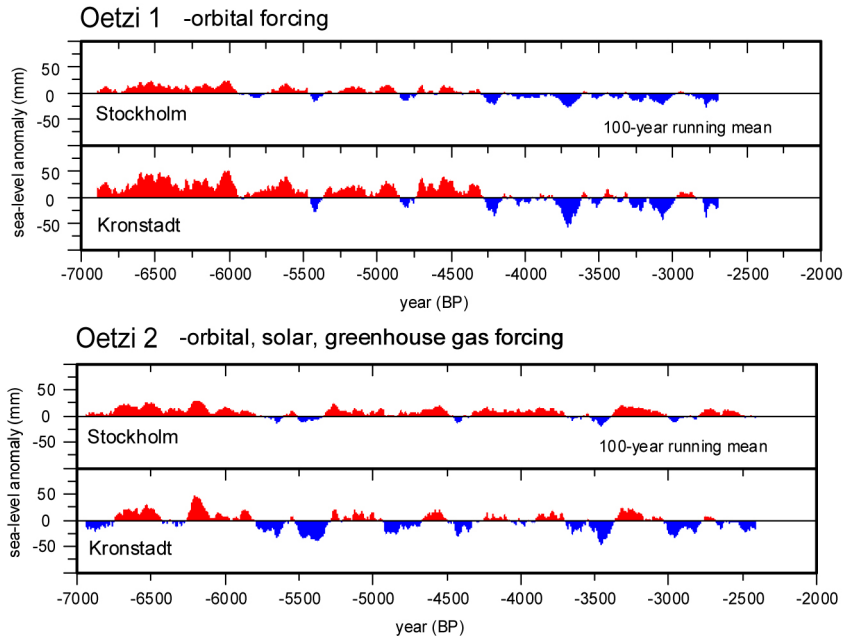

Fig. 24: *Estimation of the contribution of SLP changes to historical winter sea-level change for two stations in the Baltic Sea central based on regression between observed sea level as predictand and SLP as predictor. For the estimations, the predictors were taken from the Holocene climate simulations Oetzi 1 and Oetzi 2 with the global climate model ECHO-G. The regression model was calibrated with observations in the period 1900 to 1999. Time-series were smoothed by a 101-year low-pass filter.*

Fig. 25 displays the contribution of precipitation changes to historical winter sea level changes in two sea level stations in the south-western Baltic Coast based on regression, for Oetzi 1 and 2.

Similarly, the long-term contribution to precipitation is for a slight negative tendency in Baltic sea-level in the Southern Baltic. This is caused by a reduction of winter precipitation at these latitudes that accompanies a general climate cooling from the early Holocene to the present.

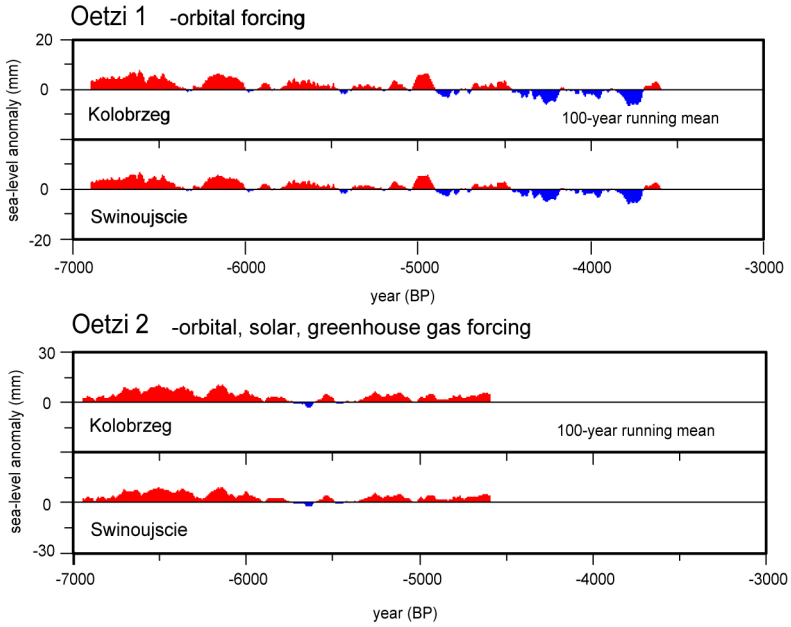

Fig. 25: *Estimations of the contribution of precipitation changes to historical winter sea-level change for two stations in the southern Baltic Sea based on regression between observed sea-level as predictand and area-averaged precipitation as predictor. For the estimations, the predictors were taken from Holocene climate simulations Oetzi 1 and Oetzi 2 with the global climate model ECHO-G. The regression model was calibrated with observations in the period 1900 to 1999. Time-series were smoothed by a 101-year low-pass filter.*

4.3.1.2 Contribution of regional climate to future winter sea-level changes

Fig. 26 shows the estimations of the contribution of changes in atmospheric forcing to future winter sea-level change in the Baltic Sea using the output of different GCM simulations.

The estimated linear trends of the contribution of SLP and precipitation changes to future winter sea-level change are given in Table 2, together with their 95% confidence interval.

For the sea-level stations Stockholm and Kronstadt (predictand SLP PCs) the simulations with the climate models HadCM3, ECHAM5 and GFDL CM 2.1 show a clear significant positive signal on sea-level rise. The strongest signal is obtained by applying the SLP output of the GFDL CM 2.1 simulation to the regression models (see Table 2 for more details).

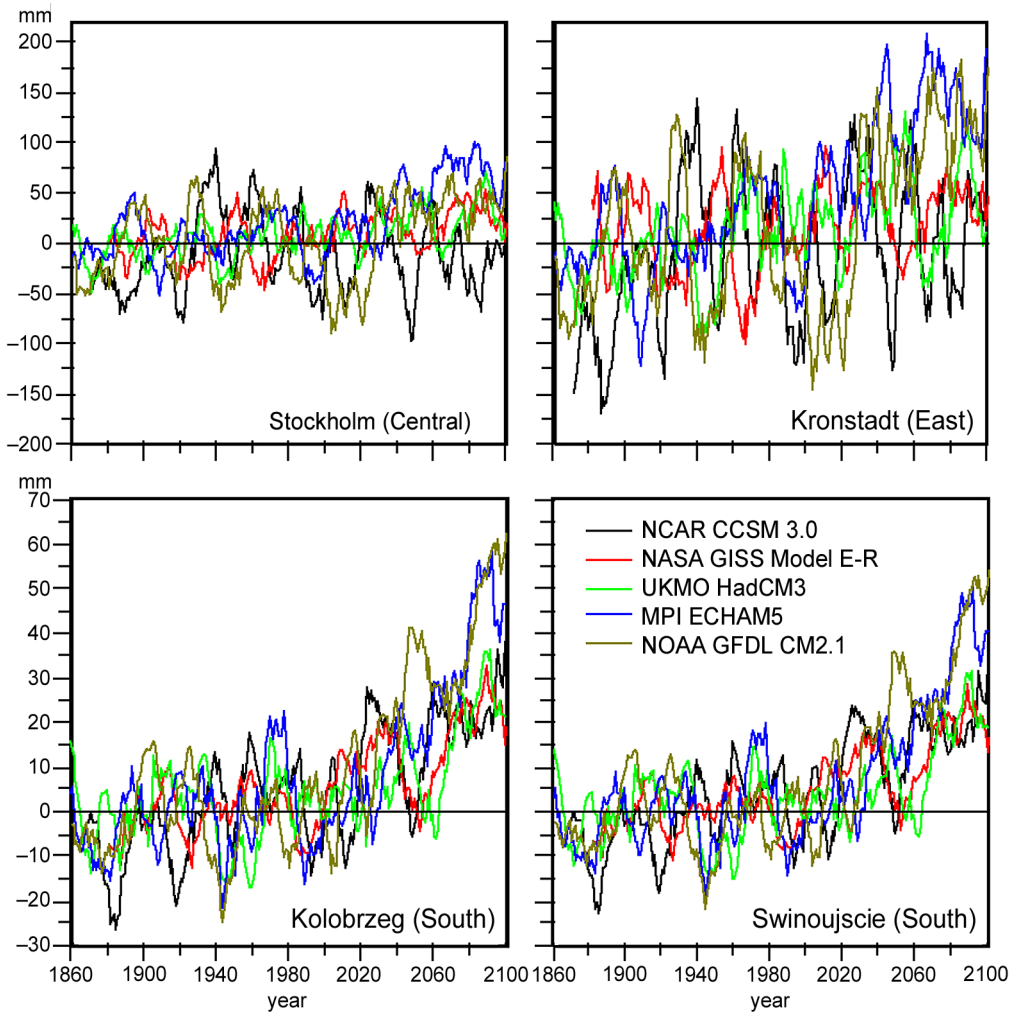

Fig. 26: *Estimations of the contribution of SLP (upper panels) and precipitation (lower panels) changes to future winter sea-level change for two stations in the central and east (upper panel) and two stations in the southern (lower panels) Baltic Sea, based on regression between observed sea-level as predictand and SLP (upper panels) and precipitation (lower panels) as predictor. For the estimations, the predictors were taken from climate simulations with the global climate models CCSM 3.0, GISS E-R, HadCM3, ECHAM5, GFDL CM 2.1, driven by IPCC SRES future scenarios of anthropogenic radiation forcing A2. The regression model was calibrated with observations in the period 1900 to 1999. Time-series were smoothed by an 11-year low-pass filter (adapted from Hünicke 2009).*

Table 2: *Estimated linear trends of the contribution of SLP and precipitation changes to future winter sea-level change (2000 to 2100), together with their 95% confidence interval (from Hünicke 2009).*

Trends mm/year (95% confidence interval)	*Kolobrzeg*	*Swinoujscie*	*Stockholm*	*Kronstadt*
Global climate models	predictor precipitation		predictor sea-level pressure	
NCAR CCSM 3.0 (POP OGCM)	0.24 (±0.05)	0.21 (±0.05)	-0.19 (±0.21)	0.01 (±0.38)
NASA GISS Model E-R (Russell OGCM)	0.17 (±0.04)	0.14 (±0.03)	0.14 (±0.09)	0.13 (±0.17)
UKMO HadCM3	0.30 (±0.05)	0.26 (±0.04)	0.32 (±0.13)	0.29 (±0.26)
MPI ECHAM5	0.60 (±0.04)	0.52 (±0.04)	0.88 (±0.13)	1.25 (±0.26)
NOAA GFDL CM 2.1	0.62 (±0.05)	0.54 (±0.04)	1.24 (±0.18)	2.53 (±0.34)

The ECHAM5 model also produces a much higher positive trend for Kronstadt than for Stockholm, but the values are lower. The HadCM3 model leads to positive trends, but much weaker and more similar between the two sea-level stations. Whereas the CCSM 3.0 model shows no significant trend for both sea-level stations, the GISS model produces a minor upward trend for Stockholm. Considering all significant values, the mean estimate changes brought about by simulated changes in the SLP field are of the order of 1 mm/year for the investigated sea-level stations for the time period 2000 to 2100.

The estimation of the contribution of precipitation changes to future winter sea-level changes in the Southern Baltic Sea level stations Kolobrzeg and Swinoujscie (predictand area-averaged precipitation) shows a much more uniform result across the simulations. Similar to the findings using SLP as predictor, the strongest signal is reached by applying the precipitation output of the GFDL CM 2.1 simulation to the regression models. Thereby the 21st century trends reach values of 0.63 ±0.05 mm/year for Kolobrzeg and 0.54 ±0.04 mm/year (95% confidence interval) for Swinoujscie. Again, the ECHAM5 model delivers quite similar results. The lowest trends are estimated by using the precipitation output of the NASA GISS Model. The results for the NCAR and UKMO climate models are quite similar. For more details read Hünicke (2009).

5 Proxy-data - Research Focus III

What is the best proxy data in the Baltic Sea Sector to ascertain the realism of the Holocene climate model simulations and how useful is this data for the particular needs of climate modelling within the Baltic Sea Region?

The realism of the presented long climate simulations in the Baltic Sea Sector has to be ascertained by comparing different key variables with adequate reconstructions based on proxy data. It is assumed that the best proxy data for this purpose are tree ring data; as such data is known to have a reasonable spatial coverage and can be dated quite accurately.

5.1 Tree ring data

Not all dendrochronological (tree ring) time series are responsive to the same climate parameter and to the same season. For instances, some dendroclimatological data might be more sensitive to temperature variations (probably those located close to the coast line) and others more indicative of variations in the hydrological cycle. As both, temperature (related to the NAO) and precipitation, have been somehow statistically found to have influence on sea-level variations in different parts of the Baltic Sea (see Chapter 3), attention was firstly devoted to both aspects of the climate sea-level relationship.

Nowadays there exist a few dendroclimatological datasets, which are generally available over the internet. Perhaps the best known is the International Tree Ring Data Bank (ITRDB)[4], operated by the NOAA Climatology Program and the World Data Center (WDC) for Paleoclimatology. Other datasets with relevance to the SINCOS project were expected to spread over different institutions and data sources, which are often barely documented for the general researcher.

[4] http://www.ncdc.noaa.gov/paleo/treering.html

5.1.1 Site selection and sample collection

In order to correctly interpret dendrochronological results, it is essential to be familiar with the characteristics of the site, as well as the factors regulating tree growth.

Tree ring samples are collected in the field by using a hand held increment borer to remove a cylinder of wood roughly 5mm in diameter along the radius of a tree. The investigator selects the site in order to maximize a particular signal. For reliable statistical analysis, a rule of thumb is around 20 trees per site. This number varies according to the strength of the climate signal in the trees and the purpose of the collection. To facilitate cross-correlation and accurate dating of the annual rings, two samples are generally collected per tree. The collected samples are then mounted and finely sanded in the laboratory. This allows cross-dating and measurement of the widths of the annual rings. In some cases wood density is also measured, which may provide a more reliable growth signal and additional information. The ring widths are measured to the nearest 0.01mm or .001mm and recorded in computerized data files.

5.1.2 Tree ring Data Sets with relevance for the Baltic Sea Region

Beside the ITRDB, a couple of European dendrochronological laboratories were found to provide open access to their databanks, for instance the SAIMA Unit of the Savonlinna Department of Teacher Education (SAIMA Unit)[5] at University of Joensuu in Finland and the Swiss Federal Institute for Forest, Snow and Landscape Research (WSL)[6]. However, the information contained in these European databanks seems already augmented in the ITRDB. Nevertheless, it was randomly tested if the data provided by ITRDB is similar –and up-to-date –comparing to the European Databanks. This was the case (in 2008).

In a next step it was analysed which of the data are might applicable for the particular needs of our study. Thus, the following selection criteria where applied: The tree ring data sets

- have to stem from sites situated within the Baltic Sea Area.

[5] http://sokl.joensuu.fi/saima/homepage3/dataa1.htm
[6] http://www.wsl.ch/dendro/dendrodb.html

- span a long time period which allow for a comparison between tree ring based reconstructions and climate simulations.
- cover an adequate period with meteorological observations.

Based on these criteria's it was decided to select only tree ring data sets which cover at least the time period 1550 to 1950. This reduced the number of possible useful tree ring data (ITRDB) to 18 tree ring data sites: 16 pine tree sites (PISY) from Finland, Norway, Russia and Sweden and 2 oak sites (QURO) from Germany and Poland. The location of these 18 data sites are shown in Fig. 27. The station details (e.g. sites, length of time series, data contributors) can be found in Table 3. The number of tree ring sites used for this study was later on reduced to 15 (see Section 5.3.3).

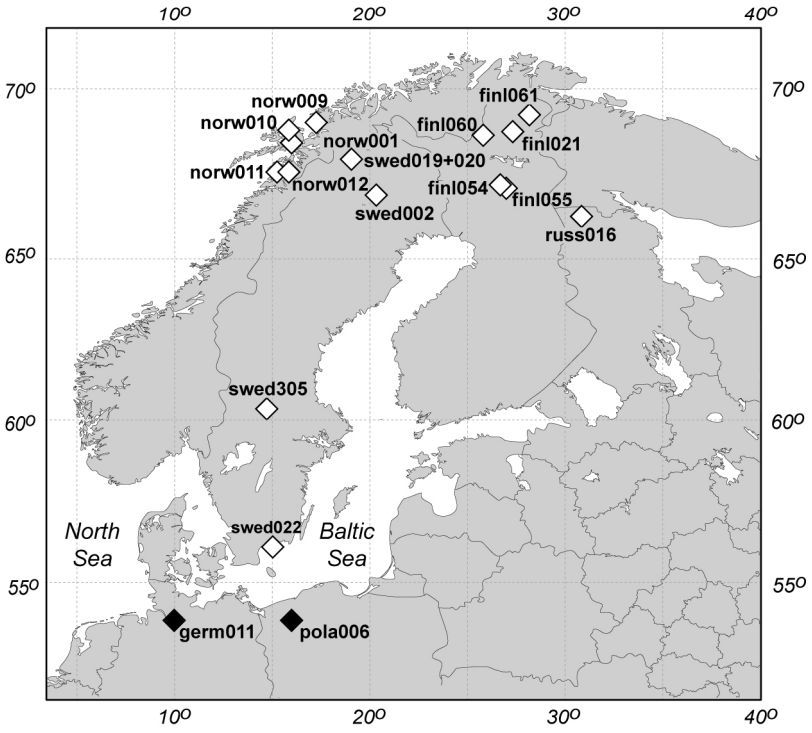

Fig. 27: *Sketch of the Baltic Sea Region, showing the locations of the ITRDB tree ring sites used in this study. The locations are indicated with the ITDRB code names. Tree ring data oak sites (QURO) are indicated with white squares, pine sites (PISY) with black squares. The full location names together with the length of the data sets and the reference to the data contributors, respectively, can be found in Table 3.*

Table 3: *List of ITRDB tree ring sites within the Baltic Sea Region used for this study, indicating the full location names, the ITRDB code names and the lengths of the data sets together with the starting year and end year. Data contributors are: Wazny (pola006), Eckstein (germ011), Jonsson (swed002), Axelson (swed305), Schweingruber (swed020, swed022, swed019, norw001), Meriläinen (russ016, finl021), Melvin (norw012, norw011, finl055, finl054), Kirchhefer (norw009, norw010), Briffa (finl060, finl061). The chronologies recorded in the ITRDB are those calculated by the original investigator. * Tree ring data sites for which the ITRDB is providing already standard chronologies beside the measured raw ring widths data are finl021, germ011, norw001, norw009, norw010, pola006, russ016, swed002, swed019, swed020, swed022 (see Section 5.3.2 for details).*

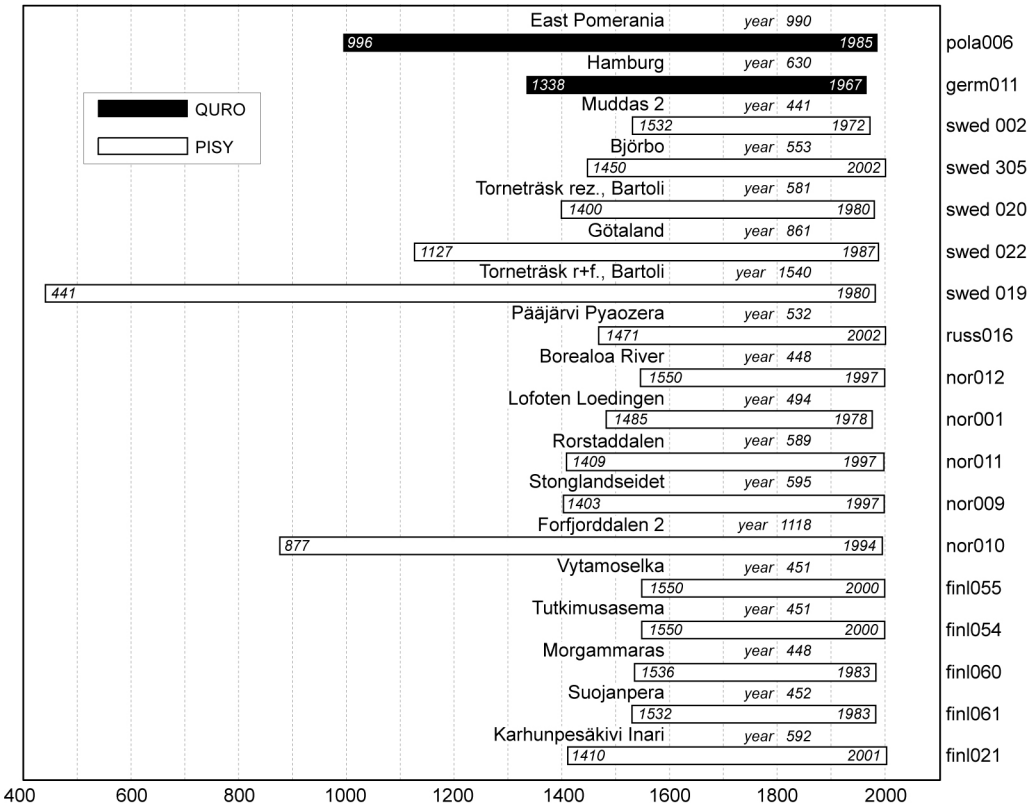

Additionally, around 27 dendrochronologists within the Baltic Sea Region were contacted; including Researchers within the countries Denmark, Germany, Estonia, Finland, Latvia, Lithuania, Norway, Poland, Russia and Sweden. Nine of them delivered information about their available dendrochronological datasets with relevance for the Baltic Sea Region, including details about geographical position, time period, tree species, measured parameters, standardisation, possible dendroclimatological analyses and publications. Finally, five out of

these nine laboratories are found to have tree ring data available which meet the selection criteria explained above. Table 4 lists the laboratories and their Institutions with contact details and a rough description of datasets. It turned out that most of these datasets are not published yet (2008). Therefore, the laboratories should be contacted directly to request more information and possible collaborations in terms of further analyses of the data.

Table 4: *List of contacted Dendrochronological Laboratories, which delivered valuable information about tree ring data sites might useful for this study. Institutions with contact details and a rough description of datasets are indicated. Note the request of information steam from a contact in summer 2007. Contacted Institutions/ Laboratories, which delivered information, but had not valuable tree ring data (>1550-1950) available at that time were: University of Cologne /Germany (B. Schmidt), University of Latvia, Riga, Latvia (M. Zunde), Vytautas Magnus University, Kaunas, Lithuania (R.Pukine), University of Szczecin, Szczecin, Poland (A. Cedro).*

Institution / Country	Contact Details
Deutsches Archäologisches Institut / Germany	Scientific Department of the Head Office, Dendrochronology,Im Dol 2-6, 14195 Berlin, http://www.dainst.org/abteilung_7064_de.html, contacted person: KU Heußner (dendro@dainst.de)
University of Hamburg/ Germany	Institute for Wood Biology and Wood Protection, Department of Wood Science, Leuschnerstr. 91, 21031 Hamburg, http://www.bfafh.de/inst4/42/index.htm, contacted person: D, Eckstein (d.eckstein@holz.uni-hamburg.de)
University of Tartu/ Estonia	Institute of Geography, Vanemuise Str. 46, 51014 Tartu, http://www.geo.ut.ee/english/index.html, contacted person: A. Läänelaid (alar.laanelaid@ut.ee)
Vytautas Magnus University/ Lithuania	Faculty of Nature Science, Environmental Research Centre, Dendroclimatology and Radiometrics Group, Z.E. Zilibero 6, 46324 Kaunas, http://www.freewebs.com/dendrochronology/adomas-en.html, contacted person: A. Vitas (a.vitas@gmf.vdu.lt)
University of Tromsø/ Norway	Department of Biology, 9037 Tromsø, contacted person: Andreas Kirchhefer (andreas.kirchhefer@ib.uit.no)

5.2 Climatic Datasets relevant for the tree ring data evaluation

The climatic datasets used for the evaluation of the tree ring data (temperature and precipitation data) were selected for single stations, situated near by the 18 tree ring data sites. The datasets were obtained via internet from the Royal Netherlands Meteorological Institute

(KNMI)[7], the Climate Research Unit (CRU)[8] of the University of East Anglia (UEA) and the Deutscher Wetterdienst (DWD)[9]. For download, the Climate Explorer[10] was used. The selection of the climatic station grids was based on the following criteria:

The climatic data sets

- cover an adequate period with dendrochronological datasets, at least >50 years.
- are situated as closest as possible to each of the 15 tree ring sites, respectively.

In case of single missing values within the time-series, the gap was filled by an interpolation value of the monthly mean over the whole length of the time-series. All climatic datasets were adapted, merged and stored as input for the evaluation of the dendrochronological datasets.

5.3 Statistical Evaluation of the tree ring data sets

5.3.1 Programs/Software

COFECHA is a quality-control program used for statistical evaluation of the crossdating and overall quality of tree-ring chronologies (Holmes 1983). A modified form of COFECHA has been run on the chronologies in the ITRDB, during two quality-control projects completed in 1996 and 2005, respectively. The program is contained in the ITRDB Program Library[11].

The Program ARSTAN (Cook 1985) is used to produce chronologies from tree-ring measurement series by detrending and indexing (standardizing) the series, before applying a robust estimation of the mean value function to remove effects of endogenous stand disturbances. The common signal is often enhanced by an autoregressive modeling of index series. An extensive statistical analysis of a common time interval provides a characterization of the data set. The software produces three versions of each chronology, intended to contain a maximum common signal and a minimum amount of noise.

7 http://climaexp.knmi.nl
8 http://www-cru.uea.ac.uk/cru/data
9 http/www.dwd.de
10 http://climexp.knmi.nl
11 http://www.ltrr.arizona.edu/pub/dpl/

DendroClim2002 is a program which involves the implementation of bootstrapped correlation and response functions to identify climatic signals in tree rings and allows the analysis of a single time period (or interval) as well as of multiple time intervals. Input data needed for this program are monthly climate variables (typically precipitation and temperature), and tree-ring index values for a given time period. After specifying the input files, the user defines window boundaries to run the analysis. Depending on input conditions, the user can run either bootstrapped correlation or response functions on a single time period (interval), or on multiple intervals. The evolutionary and moving intervals essentially iterate the bootstrapped correlation and response functions for different time periods. Each bootstrap estimate is obtained by generating 1000 samples (selected at random with replacement), then running numerical computations on each sample. Computations involve linear correlation, Jacobean rotations for Eigenvalues, singular value decomposition and solutions of linear systems accompanied by principle component regression.

5.3.2 Standardisation of the tree ring data sets and establishment of chronologies[12]

Many of the chronologies in the ITRDB were produced (including standardisation) by using the Program ARSTAN (Section 5.3.1). The chronologies recorded in the ITRDB are those calculated by the original investigator. However, the raw ring widths are also archived to allow reprocessing of the chronologies. To receive a site chronology, the raw ring width data form samples collected at one site has to be standardized and the results has to be averaged to generate a series of growth indices. This involves the fitting of a curve to the ring-width series and the dividing of each ring-width value by the corresponding curve value (or calculating the difference between the ring-width values and the curve value). Such process allows samples with large differences in growth rates to be combined, and can be used to remove any undesired growth trends present. The output – a series of standardized growth indices –can then be used to interpret a proxy environmental signal in the data. These indices are unitless and characterised by a nearly stable mean and variance, which allows for averaging indices from numerous trees into a site chronology. The statistical methods for accomplishing the standardization can be complex.

[12] http://www.ncdc.noaa.gov/paleo/treeinfo.html

The chronology represents the departure of growth for a given year vs. the series mean and representing the long term mean. Higher or lower values for a given year represent proportionally higher or lower tree growth for that year. A researcher can combine knowledge of the individual site and tree species to interpret the growth variations in terms of climate or other environmental factors.

11 out of the 18 selected tree ring data sites (Fig. 27) provide, beside the measured raw ring widths data, already standard chronologies out of it (two out of them also provided as 'white' residual chronologies). The respectively chronology sites together with the ITDRB codes are indicated in Table 3.

However, the ITRDB seem not to provide all relevant information about the standardisation process for each of the chronologies. Because of that, it was decided to reprocess the chronologies by using the raw ring widths data, which are also archived by the ITRDB.

5.3.3 Evaluation of the raw ring widths data

For the statistical evaluation, the raw ring widths data of the 18 selected sites (Fig. 27) is quality-controlled by using the program COFECHA (as explained above in Section 5.3.1). The chronologies are then produced by using the software ARSTAN. To provide a comparison of different types of chronologies, different standardisation methods are applied for each of the sites.

The own calculations with COFECHA lead partly to differences in the results to those provided by the ITRDB chronologies. In specific, this affects the chronologies out of the tree ring sites with the ITRDB codes numbers norw011, norw001, swed002, germ011 and pola006.

In three cases occur problems due to the data implementation into the software programs. Therefore, the number of further investigated chronologies was reduced to 15. Fig. 28 shows the 15 Baltic area dendro-chronologies, based on regional curve standardisation (rcs) for their overlapping time period.

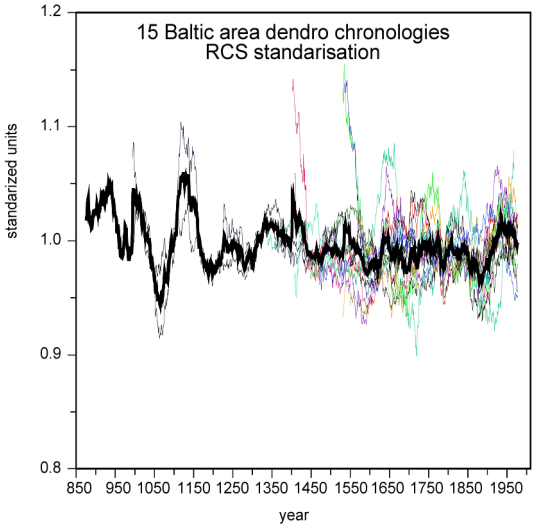

Fig. 28: *Time-series of the 15 further investigated tree ring chronologies, based on RCS standardisation, for the time period 850 to 1960, smoothed with a 31-year Gaussian mean filter. The location of the tree ring sites are indicated in Fig. 27.*

5.4 Identification of climatic signals within the tree ring chronologies

In a next step the program DendroClim was used to identify possible climatic signals in the tree ring chronologies. Therefore, the residual (res) values of the calculations with the regional curve-standardisation (rcs) method were applied. As climatic parameters, mean monthly temperature and mean monthly precipitation time series (see Chapter 2 for the different data sources) were used. The focus lied on the time span between Septembers of the previous year and Augusts of the recent year, respectively. The length and years of calculations depended on the available climatic input data. The base length for evolutionary and moving intervals was 48 years (with exception of long selected time periods). As conditions for response and correlation the selected intervals of years were set to be greater than or equal to 1.5 times as the number of predictors. For the evolutionary and moving response and correlation, the common interval was set to be greater than twice the number of predictors. More information about relevant time periods of the input data and the resulting length of time series of the DendroClim calculations as well as significant correlations and possible comments are available via request. The significant correlations between the tree ring data and climatic parameters (temperature and precipitation) are shown for each month (September to august) as absolute values in Table 5.

Table 5: *Statistically significant correlation values of the tree ring width data (residuals of regional curve standardisation (rcs-res)) and temperature (T) and precipitation (P) data series for each month (single intervals, absolute values). Calculations with DendroClim, based on selected time periods within the 20th century.*

	significant correlation values (single interval)																							selected time period
rcs-res	SEP T	OCT T	NOV T	DEC T	Jan T	Feb T	Mar T	Apr T	May T	Jun T	Jul T	Aug T	SEP P	OCT P	NOV P	DEC P	Jan P	Feb P	Mar P	Apr P	May P	Jun P	Jul P	Aug P	
finl061																									1902–1983
finl021																									1902–2000
finl060																									1902–1983
fi054																									1902–2000
fi055																									1902–2000
russ016																									1902–2000
sw002																									1902–1972
swed305																									1902–2000
no009																									1902–1997
no010																									1902–1994
no001																									1902–1978
no011																									1902–1997
no012																									1902–1997
ge011																									1902–1967
pola006																									1902–1985

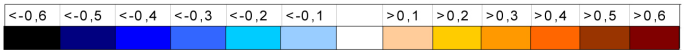

Table 5 indicates, in which of the 15 chronologies a climate signal can be identified and which months show which statistically significant correlation with one of the two climate parameters (temperature and precipitation). The results show a general tendency of spatially stronger statistically significant correlations with temperature (T), especially in the summer month with values in the range of 0.2 up to maximum values of >0.5 to 0.6 in July in 11 of the chronologies sites in Finland, Norway and Sweden.

Statistically significant correlations between precipitation (P) and tree ring width can be just identified for the chronologies in Poland and Germany for single month. For the German chronology (ge011) this regards the months November and may, which show statistically significant correlation values in a range of 0.3 to 0.4 (and for august 0.2 to 0.3). Generally, most positive statistically significant correlations with precipitation are found in the month may within 6 out of the 15 studied chronologies sites. However, the month July shows negative correlations in the range of -0.2 to -0.3 (with maximum values up to -0.4 to 0.5 in sites of Norway) in 8 of the 15 investigated chronology sites.

These points to the fact that the investigated tree ring chronologies allow only for the reconstruction of summer temperatures.

5.5 Climate conditions versus investigations sites

To get a hint about chronology sites, which possibly underlay similar climate conditions, the correlation coefficients (r) together with its square (r^2) were calculated between the single residual chronologies (res-rcs) for the countries Norway, Finland, Sweden, Germany/ Poland for time periods up to 500 years, depending on the length (overlapping time period) of the available chronologies. Thereby, the value of the square of the correlation coefficient (r^2) represents the fraction of the variation (also denoted as fraction of variance) in one variable that may be explained by the other variable. Table 6 shows the calculated correlation coefficients together with its square for the chronology sites in Finland and Norway for different time-periods.

Table 6: *Correlation\ Correlation Square matrixes ($r\backslash r^2$) of selected residual chronologies (res-rcs) for different time periods in Norway (1550 to 1978) and Finland (1550 to1983). The chronology sites are indicated through the ITRDB code name (see Table 3 for the full names). Variance values over 50 % are indicated in bold.*

r \ r²	no001	no009	no010	no011	no012
no001	**1**	0,38	0,48	0,34	0,27
no009	0,62	**1**	**0,54**	0,27	0,31
no010	0,69	0,73	**1**	36,7	0,41
no011	0,58	0,52	0,61	**1**	0,44
no012	0,51	0,55	0,64	0,66	**1**
r \ r²	finl021	finl054	finl055	finl060	finl061
finl021	**1**	0,48	**0,56**	**0,67**	**0,61**
finl054	0,69	**1**	**0,66**	0,45	0,38
finl055	0.75	0,81	**1**	**53,1**	0,42
finl060	0,82	0,67	0,73	**1**	**0,56**
finl061	0.78	0,61	0,65	0.74	**1**

It can be seen that especially most of the finish sites show a high correlation to each other, which points to a possibly similar climate influence on chronology sites within this region.

The two Swedish sites (swed002, swed305) show a low non-significant correlation (0.22) for

the investigated time-period 1532 to 1972. Also, the correlation between the two sites of the south-western Baltic (germ011, pola066) show a low value of r=0.27.

Similar calculations were done for the climatic data sets of temperature and precipitation, based on the CRU data set (see Section Data Sets). Again, it was assumed that high correlation coefficient point to sites which underlay similar climatic influences with regard to temperature and precipitation. Table 7 shows the results for the square of the correlation coefficient r^2 >60% exemplary for precipitation for each month of the year, based on the mean values within 1900 to 2000. As stated before, the climatic datasets were selected from single (grid) stations situated most near by the tree ring data sites.

Table 7: *Fraction of variances of precipitation with values r^2 >60% for different sites within the investigation area for each month of the year, based on the mean in 1900 to 2000. The site names correspond to the respectively ITRDB code names (see Table 3).*

	r^2 (%) based on the mean precipitation 1901 to 2000											
	p jan	p feb	p mar	p apr	p may	p jun	p jul	p aug	p sep	p oct	p nov	p dec
finl021–finl054	56,9	63,7	53,9	54,3	60,1	48,4	57,3	53,0	68,0	64,1	38,1	46,0
finl021–finl055	59,9	66,0	58,4	56,4	64,5	55,1	61,6	56,0	71,2	65,2	42,8	47,1
finl021–finl060	78,5	83,4	77,8	80,3	80,9	80,8	89,5	79,7	83,8	83,3	73,2	80,5
finl021–finl061	85,2	88,2	89,8	88,2	89,4	91,8	87,5	87,1	88,5	89,8	85,7	81,0
finl054–finl055	98,8	98,8	98,5	98,8	98,4	98,2	98,6	98,8	99,2	98,2	98,2	99,1
finl054–russ016	54,3	50,8	50,2	53,5	42,4	34,3	37,3	42,1	58,8	99,1	42,0	57,8
finl054–finl060	56,4	70,1	52,8	56,7	57,0	61,4	65,4	52,3	70,2	63,4	53,6	55,3
finl055–finl060	57,8	70,2	57,4	55,9	58,4	64,3	68,5	54,1	72,0	68,6	55,4	54,4
finl055–russ016	59,8	56,3	59,2	61,1	52,5	43,7	46,7	50,9	65,7	70,3	52,9	63,1
finl060–finl061	65,7	71,9	70,4	68,6	80,2	72,4	72,9	73,5	69,5	73,9	55,9	58,1
germ011–pola006	65,4	47,9	66,4	30,0	22,3	27,1	19,0	17,6	35,5	45,7	42,5	59,7
norw001–norw009	95,6	93,7	92,6	90,4	89,8	89,9	93,2	93,2	93,8	95,2	95,0	95,7
norw001–norw010	96,5	94,4	95,4	95,0	97,7	97,4	98,2	97,8	96,6	96,8	96,9	94,9
norw001–norw011	85,4	78,1	81,5	76,3	84,0	81,7	85,2	84,1	83,6	84,3	88,3	80,5
norw001–norw012	88,8	83,4	82,1	78,1	83,7	82,2	85,9	84,5	81,1	87,5	86,9	81,0
norw009–norw010	90,4	83,7	86,5	83,3	84,2	85,4	88,8	88,5	87,5	90,7	90,0	87,1
norw009–norw011	80,0	72,9	75,5	65,9	70,2	70,9	78,0	76,4	78,9	77,0	83,9	78,9
norw009–norw012	83,5	79,1	75,5	69,2	73,4	69,6	79,1	78,2	78,8	82,2	83,3	81,4
norw010–norw011	75,1	63,0	66,2	59,4	75,3	70,9	77,2	75,4	70,2	73,4	78,5	62,8
norw010–norw012	77,8	66,3	66,7	59,5	73,4	71,7	77,6	74,7	66,0	75,8	75,2	62,2
norw011–norw012	95,9	95,6	96,4	95,2	96,1	96,9	98,3	96,4	96,7	96,5	96,2	96,9

>90%	>80%	>70%	>60%

In general, the findings confirm the results obtained in the previous section with the strongest sites-correlations in Norway and Finland. The same calculation was done for the temperature data set, resulting –as expected –in even more significant correlations between the single station sites.

5.6 Summer Temperature versus winter precipitation

The data analysis with DendroClim pointed out, that the investigated tree ring chronologies allow only for the reconstruction of summer temperatures. As our main interest lies actually in the winter season and in precipitation in specific (as our final goal is the reconstruction of the decadal sea-level variability based on a transfer function between winter precipitation and sea level observations) the question about the relation between temperature and precipitation arises.

Hünicke and Zorita (2006) discussed this question in their paper about the influence of temperature and precipitation on decadal Baltic Sea-level variations and could clearly show that temperature and precipitation are negatively correlated at inter-annual to decadal timescales. Fig. 29 illustrates this relationship between precipitation and temperature in the Baltic Sea Region.

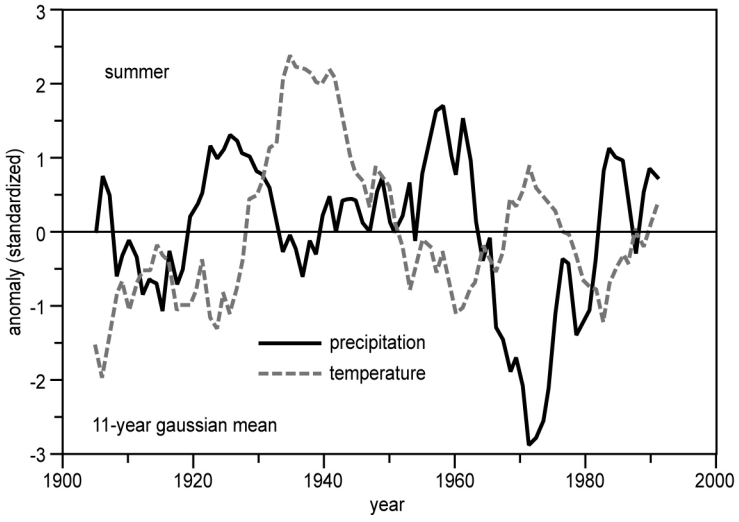

Fig. 29: *Summer (June-July-August) mean temperature and precipitation anomalies in the Baltic Sea Region, smoothed with an 11-year Gaussian mean filter, standardized to unit standard deviation. The precipitation data steam from CRU (Hulme et al. 1998) and the mean was calculated for the geographical region 11.25E to 26.25E and 52.5N to 62.5N. For the temperature data, a gridded data set of Jones and Moberg (1999) was used for the region 10E to 30E and 52.5N to 62.5N (adapted from Hünicke and Zorita 2006).*

On inter-annual timescales this anti-correlation can be might explained by the cloud cover; on longer timescales the external forcing (solar forcing) possibly come into play.

However, as the climate signal within the investigated dendro-chronological material was strongest in the month July, the relation between precipitation and temperature was also analysed for the specific grid points (near the tree ring sites) within the CRU dataset (see data sets), resulting in negative correlation coefficients.

5.7 Conclusion

A climate signal could be detected in all investigated tree ring data sets, but with a stronger sensitivity to temperature variations. This can be possibly explained by the proximity of the investigated sites to the coastline. It could be pointed out that this relation is strongest in the summer month. Thus, the investigated tree ring chronologies seem to allow only for a reconstruction of summer temperatures.

These findings unfortunately exclude the possibility to reconstruct sea-level by applying the found transfer function (see Section 3.1.1 and 4.3.1). As the main reason serves the fact that the transfer function between sea-level and climatic forcing was only found to be applicable for the winter season, as this is the season where the atmospheric forcing is found to be largest. Nevertheless, other reasons should be discussed in the following: temperature and precipitation were found to be negatively correlated with each other. Precipitation would have been served as a good predictor for reconstructing sea-level in stations of the South-western Baltic Coast. For stations outside the southern Baltic Coast, SLP (decomposed in its principal components) was found to be a good predictor. Temperature is closely related to the NAO, which is expressed through the first principal component of SLP. However, the NAO by itself would not be applicable as predictor, as it shows high in-stationeries over time and therefore does not allow for a robust result. According to Hünicke et al. (2008), at least the first three main patterns of SLP have to be taken into account as predictor in the transfer function.

6 Summary and Outlook

Baltic Sea level records show large trends due to the isostatic post-glacial rebound. Is it possible to identify the underlying influence of regional climate factors by analysing the amplitude of the annual cycle of sea-level, which is not affected by the isostasy?

Baltic Sea level records show large trends due to the isostatic post-glacial rebound. Following the statistical approach of a trend analysis of the amplitude of the seasonal cycle of Baltic Sea level, it was shown that it is possible to identify the underlying influence of regional climate factor, which is not affected by the isostaty. The results confirmed the findings of SINCOS I and supported the robustness of the former results, which were reached by an approach depend on the isostatic trend.

Thus, although future mean sea level rise will be dominated by the global signal due to global increase of temperatures, regionally non-negligible contributions, of the order of a few millimetres per year, from wind and precipitation have to be expected.

What can we learn from climate model simulations of Baltic Sea-level variations over the past decades to millennia's for future times?

The resolution of present climate models should be increased and the regional components of climate should be included to allow for a more realistic representation of the Baltic Sea. This project has shown that regional climate drivers may be important for the evolution of regional sea-level. However, it also became clear that present global and regional climate models are hindered by these limitations. Efforts to design regional atmosphere-coupled models for the Baltic Sea region should be strengthened.

What is the best proxy data in the Baltic Sea Sector to ascertain the realism of the Holocene climate model simulations and how useful is this data for the particular needs of climate modelling within the Baltic Sea Region?

The majority of proxy data available for model-proxy comparison in this region mostly allow for a reconstruction of past summer temperatures. Winter temperatures or annual mean temperatures can only be reconstructed assuming that the relationship between summer and

annual temperatures remain constant back in time, which is a bold and probably unjustified assumptions. Only recently, some proxy data based on historical documentary information provide for reconstructions of winter-spring temperatures, but these proxy records cover only the last few centuries (Zorita et al. 2010). The model-proxy comparison in this case indicates a good performance of the model in reproducing multi-decadal trends, but a tendency of the model to underestimate the natural decadal variations.

An extension of proxy data to cover the winter half year will be very useful to ascertain the realism of climate models to simulate climate changes at centennial and millennial timescales.

Acknowledgement

We would like to express our thanks to the German Research Foundation (DFG) for the financial support of the research in the frame of the Research Unit "Sinking Coasts – Geosphere, Ecosphere, and Anthroposphere of the Holocene southern Baltic Sea" (SINCOS). We are grateful to Beate Gardeike for her help with the figures. This study is part of the BALTEX program.

List of Tables

List of Figures

Bibliography

Berger, A. and Loutre, M.F. 1991. Insolation values for the climate of the last 10 million years. *Quaternary Science Reviews* 10: 297-317.

Biondi, F. Waikul, K. 2004. DENDROCLIM2002: A C++ program for statistical calibration of climate signals in tree-ring chronologies. *Computers & Geosciences* 30: 303-311.

Cook, E.R. 1985 A time-series analysis approach to tree-ring standardisation. *PhD Thesis, University of Arizona,* Tucson.

Crowley, T.J. 2000. Causes of Climate Change Over the Past 1000 Years, *Science*, v.289, pp 270-277, July 14, 2000.

Davis, B.A.S., S. Brewer, A.C. Stevenson, J. Guiot. 2003. The temperature of Europe during the Holocene reconstructed from pollen data. *Quaternary Science Reviews* 22: 1701-1716. doi:10.1016/S0277-3791(03)00173-2.

Etheridge, D. M., L. P. Steele, R. L. Langenfelds, R. J. Francey, J.-M. Barnola, and V. I. Morgan. 1996. Natural and anthropogenic changes in atmospheric CO_2 over the last 1000 years from air in Antarctic ice and firn, *J. Geophys. Res.* 101(D2), 4115–4128.

Flückiger, J., E. Monnin, B. Stauffer, J. Schwander, T.F. Stocker, J. Chappellaz, D. Raynaud, and J.-M. Barnola, High resolution Holocene N_2O ice core record and its relationship with CH_4 and CO_2, *Glob. Biogeochem. Cycles* 16 (1), 1010, doi: 10.1029/2001GB001417, 2002.

Gouirand, I. A. Moberg and E. Zorita. 2007. Climate variability in Scandinavia for the past millennium simulated by an atmosphere-ocean general circulation model. *Tellus* 59, 30-49.

Holmes, R.L. 1983. Computer-assisted quality control in tree-ring dating and measurement. *Tree-Ring Bulletin* 43:69-78.

Hünicke, B. 2009. Contribution of regional climate drivers on future winter sea-level changes in the Baltic Sea estimated by statistical methods and simulations of climate models. *International Journal of Earth Sciences*, doi: 10.1007/s00531-009-0470-0.

Hünicke, B., J. Luterbacher, A. Pauling and E. Zorita. 2008. Regional differences in winter sea-level variations in the Baltic Sea for the past 200 years. *Tellus* 60A (2), 384-393, doi: 10.1111/j.1600-0870.2007.00298.x.

Hünicke, B. and E. Zorita. 2008. Trends in the amplitude of Baltic Sea level annual cycle. *Tellus* 60A (1), 154-164, doi: 10.1111/j.1600-0870.2007.00277.x.

Hünicke, B. and E. Zorita. 2007. Estimation of the influence of regional climate influence on the recent past and future sea-level changes in the Baltic Sea with statistical methods and simulations of climate models. In: SINCOS -Sinking Coasts. Geosphere, Ecosphere and Anthroposphere of the Holocene Southern Baltic Sea. *Berichte der RGK* 88, in press.

Hünicke, B. and E. Zorita. 2006. Influence of temperature and precipitation on decadal Baltic Sea level variations in the 20th century. *Tellus* 58A (1), 141-153, doi: 10.1111/j.1600-0870.2006.00157.x.

Legutke, S. and R.Voss. 1999. The Hamburg Atmosphere –Ocean Coupled Circulation Model ECHO-G. *Technical Report* No. 18, DKRZ, Hamburg.

Meier, H.E.M, B. Broman and E. Kjellström. 2004. Simulated sea level in past and future climates of the Baltic Sea. *Clim Res*, 27, 59-75.

Meyer, M., J. Harff, L. Tiepolt and C. Dyt. 2009. Modelling historical coastline change with SEDSIM: The development of the Darss-Zingst peninsula since 1696 AD. *Proceedings of the International Conference on Climate Change*, 25-28 May 2009, University of Szczecin, Poland, ISSN 1681-6471.

Min, S. K., S. Legutke, A. Hense, W.T. Kwon.2005b. Internal variability in a 1000-yr control simulation with the coupled climate model ECHO-G-I. Near-surface temperature, precipitation and mean sea level pressure. *Tellus* 57A, 622-640.

Mitchell T.D. and Jones, P.D. 2005. An improved method of constructing a database of monthly climate observations and associated high-resolution grids. *Int. J. Climatol.* **25**, 693-712.

Otto, J., T. Raddatz, M. Claussen, V. Brovkin and V. Gayler. 2009. Seperation of atmosphere-ocean-vegetation feedbacks and synergies for mid-Holocene climate. *Geophys. Res. Letters* 36, L09701, doi: 10.1029/2009GL037482.

Raible, C.C., T.F. Stocker, M. Yoshimori, M. Renold, U. Beyerle, C. Casty, and J. Luterbacher, 2005. Northern Hemispheric trends of pressure indices and atmospheric circulation patterns in observations, reconstructions, and coupled GCM simulations, *J. Climate* 18, 3968-3982.

Schenk, F., D. Hansson, S.Wagner and E. Zorita. 2009. Non-stationarities in the circulation-climate-relationship over the Baltic Sea and its effects on reconstructions of climate indices. *Proceedings of the International Conference on Climate Change*, 25-28 May 2009, University of Szczecin, Poland, ISSN 1681-6471.

Schmölcke, U. 2008. Holocene environmental changes and the seal (Phocidae) fauna of the Baltic Sea: coming, going and staying. *Mammal Review* 38 (4), 231-246.Doi:10.1111/j.1365-2907.2008.00131.x

Solanki, S.K., I. G. Usoskin, B. Kromer, M. Schüssler, and J. Beer. 2004. Unusual activity of the Sun during recent decades compared to the previous 11,000 years. *Nature* Vol. 431, No. 7012, pp. 1084 – 1087.

Stuiver M., Reimer P., Bard E., Beck J., Burr G., Hughen H., Kromer B., McCormac G., Van der Plicht J., Spurk M. 1998. Intcal98 radiocarbon age calibration, 24,000-0 cal.BP, *Radiocarbon* Vol.40, No.3 (1998) 1041-1083.

Roeckner E., K. Arpe, L. Bengtsson, M. Christoph, M. Claussen, L. Dümenil, M. Esch, M. Giorgetta, U. Schlese, U. Schulzweida. 1996. The atmospheric general circulation model ECHAM4: model description and simulation of present-day climate. *Technical Report* No. 218, MPI-M, Hamburg.

Storch, H. von, E. Zorita and F. González-Rouco. 2009. Relationships between global mean sea-level and global mean temperature and heat-flux in a climate simulation of the past millennium. *Ocean Dynamics*, 58, 227-236, DOI 10.1007/s10236-088-0142-9.

Storch, H. von, E. Zorita, J. M. Jones, Y. Dmitriev. F. González and S. F. B. Tett. 2004. Reconstructing past climate from noisy data. *Science* 306, 679-682.

Terray, L., S. Valcke, A. Piacentini. 1998. The OASIS Coupler User Guide, Version 2.2. *Technical Report* 253, TR/CMGC/98-05, CERFACS.

Trenberth, K and Paolino, D.A. 1980. The Northern Hemisphere sea-level pressure data set: trends, errors and discontinuities. *Mon. Weather Rev.* **108**, 855-872.

Wolff, J., E. Maier-Reimer, S. Legutke. 1997. The Hamburg Primitive Equation Model HOPE. In: *Technical Report* No. 8, Germany Climate Computer Center (DKRZ), Hamburg.

Wagner, S., M. Widmann, J. Jones, T. Haberzettl, A. Lücke, C. Mayr, C. Ohlendorf, F. Schäbitz and B. Zolitschka, 2007. Transient simulations, empirical reconstructions and forcing mechanisms for the Mid-Holocene hydrological climate in Southern Patagonia. Climate Dynamics 29, 333-355, doi:10.1007/s00382-007-0229-x.

Weber S., T.J. Crowley and van der Schrier, G. 2004. Solar irradiance forcing of centennial climate variability during the Holocene. *Clim Dynam* 22, 539-553.

Zorita, E., S. Wagner, F. Gonzalez-Rouco and H. von Storch. 2007. Climate simulations of the Past Millenium with the Global Model ECHO-G: Results for the Baltex Area. *Proceedings of the Fifth Study Conference on BALTEX*, 4-8 June 2007, Kuressaare, Saaremaa, Estonia, ISSN 1681-6471.

Zhang, W., J. Harff and C. Wu. 2009. A long-term morphodynamic model and its application to the southern Baltic coast. *Proceedings of the International Conference on Climate Change*, 25-28 May 2009, University of Szczecin, Poland, ISSN 1681-6471.

Zorita, E., von Storch, H., González-Rouco, F., Cubasch, U., Luterbacher, J., Legutke, S., Fischer-Bruns, I. and Schlese, U. 2004. Climate evolution in the last five centuries simulated by an atmosphere- ocean model: global temperatures, the North Atlantic Oscillation and the Late Maunder Minimum. *Meteorologische Zeitschrift* 13, 271-289.

Zorita, E., Moberg, A., Leijonhufvud, L., Wilson, R., Brázdil, R., Dobrovolný, P., Luterbacher, J., Böhm, R., Pfister, Ch., Glaser, R. Söderberg, J., González-Rouco, F. 2010. European temperature records of the past five centuries based on documentary information compared to climate simulations. *Climatic Change*, in press.